

MÖBIUS DECONVOLUTION ON THE HYPERBOLIC PLANE WITH APPLICATION TO IMPEDANCE DENSITY ESTIMATION

BY STEPHAN F. HUCKEMANN¹, PETER T. KIM²,
JA-YONG KOO³ AND AXEL MUNK⁴

*Georg-August-Universität Göttingen, University of Guelph, Korea
University
and Georg-August-Universität Göttingen*

Dedicated to Dennis M. Healy Jr. 1957–2009

In this paper we consider a novel statistical inverse problem on the Poincaré, or Lobachevsky, upper (complex) half plane. Here the Riemannian structure is hyperbolic and a transitive group action comes from the space of 2×2 real matrices of determinant one via Möbius transformations. Our approach is based on a deconvolution technique which relies on the Helgason–Fourier calculus adapted to this hyperbolic space. This gives a minimax nonparametric density estimator of a hyperbolic density that is corrupted by a random Möbius transform. A motivation for this work comes from the reconstruction of impedances of capacitors where the above scenario on the Poincaré plane exactly describes the physical system that is of statistical interest.

1. Introduction. The recovery of objects, for example, densities and functionals thereof, based on noisy indirect observations, otherwise known as statistical inverse problems (see, e.g., [23]), is scientifically of intense interest. The literature is vast and we mention only a few selected papers. Most

Received October 2009; revised December 2009.

¹Supported by DFG Grant MU 1230/10-1 and GRK 1023.

²Supported by NSERC Discovery Grant 46204.

³Supported by National Research Foundation of Korea Grant 2009-0075827.

⁴Supported by DFG Grant SFB 755 and FOR 916.

AMS 2000 subject classifications. Primary 62G07; secondary 43A80.

Key words and phrases. Cayley transform, cross-validation, deconvolution, Fourier analysis, Helgason–Fourier transform, hyperbolic space, impedance, Laplace–Beltrami operator, Möbius transformation, special linear group, statistical inverse problems, upper half-plane.

| |
|--|
| <p>This is an electronic reprint of the original article published by the Institute of Mathematical Statistics in <i>The Annals of Statistics</i>, 2010, Vol. 38, No. 4, 2465–2498. This reprint differs from the original in pagination and typographic detail.</p> |
|--|

of the work is concerned with deconvolution on Euclidean spaces. Prominent approaches are based on wavelet and wavelet-vagulette expansions (see [1, 24] and [39]) or, on singular value decompositions (see [5, 26] and [33]), where for the latter block thresholding techniques lead to adaptive estimators (see [8]). Minimax rates in deconvolution have been investigated by Fan [15], and many others. Recently, oracle inequalities have been proved in [9]. The specific problem of boxcar deconvolution and its link to Diophantine approximation have been investigated in [21] and [22]. Other methods include the linear functional strategy (see [16] and variants thereof). Very popular are Fourier series estimators which have been known for a long time, and often they become particularly simple because on Euclidean spaces they can be treated with kernel methods (see [15, 19] and [44]). We note that even though our approach also utilizes Fourier methods on groups, due to the hyperbolic geometry, the resulting estimator cannot be treated by kernel methods thus complicating our endeavor considerably.

In this paper we provide a novel methodology for statistical object recovery on the Poincaré upper half plane which we call the problem of Möbius deconvolution. Here the group of Möbius transformations is given by all fractions of the form $(az + b)/(cz + d)$ for a complex number z and a 2×2 matrix with real entries a, b, c, d of determinant 1. The metric which is invariant under these transformations is the hyperbolic metric (to be specified in the next section) which will replace the Euclidean metric in a natural way. In fact, a key observation is that this problem can be tackled by generalized Fourier methods similar in spirit to the Euclidean case. The development of the theory builds on the foundations laid out in [43], Chapter 3. However, extending Euclidean arguments to this manifold is challenging since the hyperbolic space is noncompact, the (hyperbolic) geometry is non-Euclidean and the group of Möbius transformations is noncommutative. A fundamental technical difficulty comes from a lack of a dilation property that does not extend over from the Euclidean case. Despite these difficulties, a generic element is the Riemannian structure on a manifold, on which a Laplacian can then be defined. This together with the generic Euclidean approach as outlined in [33] will be the foundation to what will be presented below.

In addition to the theoretical interest of this novel scenario of Möbius deconvolution, there are important practical applications as well. One particular situation occurs in alternating current circuit analysis and design whenever signals travel through circuit elements as well as whenever geometries of waveguides change. A simple example of the latter is a connector to a coaxial cable, say. Here, the so-called “reflections” are modeled on the complex unit disk and the corresponding “impedances” occur in a complex half plane. Usually, these reflections or impedances are not directly visible but observed through other electrical devices, such as a “two-port” which in turn is modeled by Möbius transformations. In particular, a class of so-called

“lossless” two-ports can be identified with 2×2 matrices of determinant 1. One particular aspect of Möbius deconvolution is related to the temporal decay of impedances of capacitors whereby the above scenario on the Poincaré plane exactly describes the physical system that is of statistical interest. Other applications include the field of electrical impedance spectroscopy, as well as electrical impedance tomography. In the former, measuring varying impedances due to variable ion transport through biological membranes is currently of high interest in view of pharmaceutical drug design (see [14] as well as [41]). In the latter, in a noninvasive and radiation-free way, medical imaging can be cost effectively accomplished by measuring skin-impedances (cf. [6]). Indeed, for successful reconstruction, control of various errors is of paramount importance (see [17]). There is also work in higher-dimensional hyperbolic spaces with respect to medical imaging (see, e.g., [29]).

In statistics there is also some recognition of the Poincaré plane and its hyperbolic geometry particularly so because the parameter space of the Gaussian distribution (with unknown mean and standard deviation) is this space. Furthermore, it has been shown by several authors that the Riemannian metric derived from the Fisher information is exactly hyperbolic (see [25, 32] for details). Obviously, location and dispersion parameters of arbitrary distributions and random estimators thereof can be viewed within the Poincaré plane. Curiously here, the family of Cauchy distributions play a specific role as being equivariant under Möbius transformations (see [34, 35] for this and its consequences for parameter estimation). Based on the above, techniques from the hyperbolic geometry of the Poincaré plane are developed exclusively from a parametric point of view (cf. [36]). As far as the authors are aware, our contribution is the first attempt at nonparametric developments.

We now summarize the paper. Section 2 is a preliminary section which introduces the notation along with the Helgason–Fourier analysis needed for this paper. Following this, Section 3 presents the main results. In Section 4 we focus on computational aspects of Möbius deconvolution illustrating the ideas through simulations. To this end we introduce in addition to the hyperbolic Gauss the hyperbolic Laplace distribution. In Section 5 we go into explicit detail with respect to the Möbius deconvolution problem for statistically recovering the temporal decay of impedances of capacitors as outlined two paragraphs above. We will briefly sketch the background; however, if the reader is well versed in this field, then one can start from Section 5.4 where we examine a data set that was acquired through collaboration with the University of Applied Sciences (Fulda, Germany) that depicts the physical system of this paper. In particular, we are able to identify random impedances when only their impedances viewed through random capacitive two-ports are given. Following this, technical details of the Poincaré upper half plane and the proofs of the main theorems are collected in Appendices A and B.

As usual for two function g and f , write $f \asymp g$ if $f(x) = O(g(x))$ and $g(x) = O(f(x))$ for $x \rightarrow \infty$ or $x \rightarrow 0$, depending on context.

2. Preliminaries. In the following let \mathbb{R} and \mathbb{C} denote the real and complex numbers, respectively. Furthermore, the group of real 2×2 matrices of determinant one is denoted by

$$(2.1) \quad \mathrm{SL}(2, \mathbb{R}) := \left\{ g = \begin{pmatrix} a & b \\ c & d \end{pmatrix} : a, b, c, d \in \mathbb{R}, ad - bc = 1 \right\}.$$

This defines the group of *Möbius transformations* $M_g: \mathbb{C} \rightarrow \mathbb{C}$ by setting for each $g \in \mathrm{SL}(2, \mathbb{R})$,

$$(2.2) \quad M_g(z) := \frac{az + b}{cz + d},$$

where $M_g M_h = M_{gh}$ for $g, h \in \mathrm{SL}(2, \mathbb{R})$. Let

$$(2.3) \quad \mathbb{H} := \{z \in \mathbb{C} : \mathrm{Im}(z) > 0\}$$

be the upper half plane where “ $\mathrm{Re}(z)$ ” and “ $\mathrm{Im}(z)$ ” denote the real and imaginary parts of a complex number z , respectively. Then for each $g \in \mathrm{SL}(2, \mathbb{R})$, the Möbius transformation M_g is a bijective selfmap of \mathbb{H} . Moreover, for arbitrary $z, z' \in \mathbb{H}$ there exists a (in general not unique) $g \in \mathrm{SL}(2, \mathbb{R})$ such that $z' = M_g(z)$.

The action of $\mathrm{SL}(2, \mathbb{R})$ on \mathbb{H} , which is rather involved, is further discussed in Appendix A. It will be used in the proof of the lower bound in Appendix B.3. For the following we note that Möbius transformations preserve the family of vertical lines and circles centered at the real axis (cf. Figure 1). This is a consequence of the fact, that Möbius transformations leave the cross ratio

$$c(z_1, z_2, w_1, w_2) = \frac{(z_1 - w_1)(z_2 - w_2)}{(z_1 - z_2)(w_1 - w_2)}$$

invariant. For a detailed introduction (cf. Nevanlinna and Paatero [38], Chapter 3).

The deconvolution, or statistical inverse problem of reconstructing the density of a random object X on \mathbb{H} , of which we only see a version Y corrupted by an independent random error ε on $\mathrm{SL}(2, \mathbb{R})$ can now be formulated as

$$(2.4) \quad Y = M_\varepsilon(X).$$

A natural geometry for (2.4) is the given by the *hyperbolic distance* on \mathbb{H}

$$d(z, z') = \log \frac{1 + \sqrt{|c(z, \bar{z}', z', \bar{z})|}}{1 - \sqrt{|c(z, \bar{z}', z', \bar{z})|}}$$

since for this distance the space of isometries of \mathbb{H} is precisely the group of Möbius transformations, meaning that $d(M_g(z), M_g(z')) = d(z, z')$ for all $g \in \mathrm{SL}(2, \mathbb{R})$ and $z, z' \in \mathbb{H}$. Here, $\bar{z} = x - iy$ denotes the complex conjugate of $z = x + iy$. The corresponding *hyperbolic measure* is chosen such that:

- (i) its area element dz agrees with the area element $dx dy$ of Lebesgue measure at $z = i$, and
- (ii) it is invariant under Möbius transformations.

In consequence, the Radon–Nikodym derivative of the hyperbolic area element with respect to the Lebesgue area element at $w = u + iv$ is given by v^{-2} which is the determinant of the Jacobian

$$\begin{pmatrix} u_x & u_y \\ v_x & v_y \end{pmatrix}$$

of a Möbius transformation M yielding $M(i) = (ai + b)/(ci + d) = u + iv$. This can be verified with the complex derivative $M'(i) = (ci + d)^{-2} = u_x + iv_x$ and the Cauchy differential equations $u_y = -v_x, v_y = u_x$; cf. Terras [43], Chapter III.

At $z = x + iy \in \mathbb{H}$ we have hence the hyperbolic area element

$$(2.5) \quad dz := \frac{dx dy}{y^2}.$$

In addition, in order to properly define below in (2.6) a convolution of a density on \mathbb{H} with a density on $\mathrm{SL}(2, \mathbb{R})$, a compatible bi-invariant Haar measure dg on $\mathrm{SL}(2, \mathbb{R})$ is chosen in Appendix A.

Hence, X and Y are random complex numbers in the upper half plane \mathbb{H} equipped with the hyperbolic geometry, and ε is a random isometric self-map of \mathbb{H} applied to X by (2.2). The problem of the *Möbius deconvolution* can be made precise as follows. A density on the upper complex half plane with respect to the hyperbolic measure is called a hyperbolic density. Densities on $\mathrm{SL}(2, \mathbb{R})$ are taken with respect to the Haar measure dg .

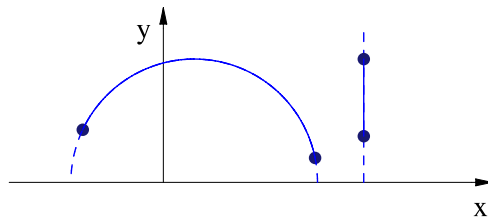


FIG. 1. The shortest connection (a geodesic segment) between two points $z, z' \in \mathbb{H}$ in the hyperbolic geometry is either a vertical line segment [if $\mathrm{Re}(z) = \mathrm{Re}(z')$] or an arc on the circle through z and z' with center on the real axis.

PROBLEM 2.1. Under the model (2.4) estimate nonparametrically, the hyperbolic density f_X of X from the hyperbolic density f_Y of Y when the density f_ε on $\mathbb{SL}(2, \mathbb{R})$ is known.

We note that this setup assumes underlying i.i.d. X_1, \dots, X_n corrupted by i.i.d. errors $\varepsilon_1, \dots, \varepsilon_n$, also independent of X_j ($j = 1, \dots, n$) giving observations $Y_j = M_{\varepsilon_j}(X_j)$, $j = 1, \dots, n$.

We will base our work using Fourier or singular value decomposition methods that are common for the Euclidean case (see [5, 26] and [33]) and the fact that the densities of (2.4) are related by the convolution

$$(2.6) \quad f_Y(z) = (f_\varepsilon * f_X)(z) =: \int_{\mathbb{SL}(2, \mathbb{R})} f_\varepsilon(g) f_X(M_{g^{-1}}(z)) dg.$$

This fact is a consequence of (A.4) in Appendix A.

From here on, we will make the abbreviation $\mathbb{SL}(2) := \mathbb{SL}(2, \mathbb{R})$, as well as to write (2.2) as simply $g(z)$ or gz for $g \in \mathbb{SL}(2)$ and $z \in \mathbb{H}$ whenever the context is clear.

2.1. *Fourier analysis on the Poincaré plane.* For purposes of Möbius deconvolution for Problem 2.1 we sketch the Helgason formulation of hyperbolic Fourier calculus which can be found in more detail in [43], Chapter 3.2. The *Helgason–Fourier* transform of $f \in C_c^\infty(\mathbb{H})$ with the latter being the space of real valued functions with compact support in \mathbb{H} with derivatives of all orders, is defined as the function

$$\mathcal{H}f(s, k) := \int_{\mathbb{H}} f(z) (\operatorname{Im}(k(z)))^{\overline{s}} dz$$

analytic for $(s, k) \in \mathbb{C} \times \mathbb{SO}(2)$ where overline denotes complex conjugation. Here,

$$k = k_u = \begin{pmatrix} \cos u & \sin u \\ -\sin u & \cos u \end{pmatrix} \in \mathbb{SO}(2) \subset \mathbb{SL}(2)$$

is naturally identified with $u \in [0, 2\pi)$ acting on \mathbb{H} as the Möbius transformation

$$M_k(z) = \frac{z \cos u + \sin u}{\cos u - z \sin u}$$

as defined in (2.2) (cf. Appendix A). Note that for all $s \in \mathbb{C}$, $z = x + iy \rightarrow y^s$ and $z \rightarrow (\operatorname{Im}(k(z)))^s$ are eigenfunctions with corresponding eigenvalues $s(s-1)$ of the Laplace–Beltrami operator

$$(2.7) \quad \Delta = y^2 \left(\frac{\partial^2}{\partial x^2} + \frac{\partial^2}{\partial y^2} \right)$$

on \mathbb{H} . With the *spectral measure*

$$d\tau = \frac{1}{8\pi^2} t \tanh(\pi t) dt du$$

on $\mathbb{R} \times \mathbb{S}\mathbb{O}(2)$ the *inverse Helgason–Fourier transform* is given by

$$(2.8) \quad f(z) = \int_{t \in \mathbb{R}} \int_{u=0}^{u=2\pi} \mathcal{H}f\left(\frac{1}{2} + it, k_u\right) (\operatorname{Im}(k(z)))^{1/2+it} d\tau,$$

where $i^2 = -1$. The following result justifies these definitions: mapping to the Helgason–Fourier transform extends to an isometry $L^2(\mathbb{H}, dz) \rightarrow L^2(\mathbb{R} \times \mathbb{S}\mathbb{O}(2), d\tau)$; that is, we have the *Plancherel identity*

$$(2.9) \quad \int_{\mathbb{H}} |f(z)|^2 dz = \int_{t \in \mathbb{R}} \int_{u=0}^{u=2\pi} \left| \mathcal{H}f\left(\frac{1}{2} + it, k_u\right) \right|^2 d\tau,$$

where we denote the space of square integrable functions over some space by L^2 . We note that $f \in L^2(\mathbb{H}, dz)$ is $\mathbb{S}\mathbb{O}(2)$ -invariant if and only if $\mathcal{H}f \in L^2(\mathbb{R} \times \mathbb{S}\mathbb{O}(2), d\tau)$ is $\mathbb{S}\mathbb{O}(2)$ -invariant. Thus, for numerical computations ([43], pages 141 and 149) for an $\mathbb{S}\mathbb{O}(2)$ -invariant function f , transforms and inverse transforms can be considerably simplified

$$(2.10) \quad \begin{aligned} \mathcal{H}f\left(\frac{1}{2} + it\right) &= 2\pi \int_0^\infty f(e^{-r}i) P_{-1/2+it}(\cosh r) \sinh r dr, \\ f(e^{-r}i) &= \frac{1}{4\pi} \int_{-\infty}^\infty \mathcal{H}f\left(\frac{1}{2} + it\right) P_{-1/2+it}(\cosh r) t \tanh(\pi t) dt \end{aligned}$$

with the Legendre function

$$P_a(c) := \frac{1}{2\pi} \int_0^{2\pi} (c + \sqrt{c^2 - 1} \cos(\phi))^a d\phi.$$

Throughout this work we will use the following assumptions:

(D.1) all densities are square-integrable

$$f_X, f_Y \in L^2(\mathbb{H}, dz), \quad f_\varepsilon \in L^2(\mathbb{S}\mathbb{L}(2), dg);$$

(D.2) the error density f_ε is bi-invariant

$$f_\varepsilon(agb) = f_\varepsilon(g) \quad \forall g \in \mathbb{S}\mathbb{L}(2), a, b \in \mathbb{S}\mathbb{O}(2);$$

(D.3) $f_X \in \mathcal{F}_\alpha(Q)$ for a Sobolev ball

$$\mathcal{F}_\alpha(Q) = \{f \in L^2(\mathbb{H}, dz) : \|\Delta^{\alpha/2} f\|^2 \leq Q\}$$

with $\alpha > 1$ and $Q > 0$.

Here, $\Delta^{\alpha/2}f$ denotes the unique function $h \in L^2(\mathbb{H}, dz)$ with $\mathcal{H}h(s, k) = \frac{1}{s(s-1)^{\alpha/2}} \mathcal{H}f(s, k)$.

As detailed in Appendix A, the isometry $\mathbb{S}\mathbb{L}(2)/\mathbb{S}\mathbb{O}(2) \rightarrow \mathbb{H}: g\mathbb{S}\mathbb{O}(2) \mapsto M_g(i)$ preserves the action of $\mathbb{S}\mathbb{L}(2)$. Hence a density f_ε satisfying (D.2) can be regarded as an $\mathbb{S}\mathbb{O}(2)$ -invariant mapping $\mathbb{H} \rightarrow \mathbb{R}$. In particular, in case of (D.1) and (D.2), the Helgason–Fourier transform $\mathcal{H}f_\varepsilon(z)$ is well defined, we have

$$(2.11) \quad \mathcal{H}f_Y(s, k) = \mathcal{H}(f_\varepsilon * f_X)(s, k) = \mathcal{H}f_\varepsilon(s) \cdot \mathcal{H}f_X(s, k);$$

[43], page 149. One final assumption to be made is the following.

(D.4) \exists constants $\beta, \gamma, C_1, C_2 > 0$ such that

$$C_1 \exp\left\{-\frac{|s|^\beta}{\gamma}\right\} \leq |\mathcal{H}f_\varepsilon(s)| \leq C_2 \exp\left\{-\frac{|s|^\beta}{\gamma}\right\} \quad \forall s = \frac{1}{2} + it, \quad t \in \mathbb{R}.$$

As an example, the hyperbolic Gaussian-distribution (see Section 3 below) satisfies (D.4).

Of course, any density on the upper half plane (or on the unit disk) can be rescaled with respect to hyperbolic measure. One example, using the normalized squared absolute cross ratio $c(z, \bar{\theta}, \bar{z}, \theta)$, has been kindly provided by one of the referees,

$$\frac{1}{\pi} \left(\frac{|z - \bar{z}| |\theta - \bar{\theta}|}{|z - \bar{\theta}|^2} \right)^2 dz = \frac{4\sigma^2 dx dy}{\pi((x - \mu)^2 + (y + \sigma)^2)^2}, \quad z = x + iy \in \mathbb{H},$$

with a hyperbolic parameter $\theta = \mu + i\sigma \in \mathbb{H}$; for example, one could take x and y as suitable estimators of the location and dispersion parameters of another distribution (cf. [34, 35]). Note that this density is not $\mathbb{S}\mathbb{L}(2)$ -invariant; rather it is equivariant with respect to the $\mathbb{S}\mathbb{L}(2)$ action on both variable z and parameter θ . In the context of this research one is interested also in $\mathbb{S}\mathbb{L}(2)$ -invariant densities. Such can be generated from suitable densities on $y \in [1, \infty)$. Moreover, $\mathbb{S}\mathbb{L}(2)$ -invariant functions additionally fulfilling (D.3) can be obtained by applying the inverse Helgason transform (2.10) to suitable functions on $s = \frac{1}{2} + it$, $-\infty < t < \infty$. If the function is even in t , then the inverse Helgason transform thus obtained is real. It is, however, not necessarily nonnegative. As a consequence of $P_{-1/2+it}(\cosh r) > 0$ for $t = 0$, nonnegativity can be obtained if the function tends sufficiently fast to zero as $t \rightarrow \infty$. Numerical experiments indicate that one may consider for $\tau > -1/4$ and $\alpha > 1$ a suitable multiple of a power of a Cauchy density in the spectral domain

$$(2.12) \quad \mathcal{H}h_{\alpha, \tau}(s, k) \propto \frac{1}{(\tau - s(s-1))^\alpha} = \frac{1}{(\tau + 1/4 + t^2)^\alpha}$$

giving an invariant *hyperbolic Laplace density* $h_{\alpha,\tau} \in \mathcal{F}_\alpha(Q)$. This density can be lifted as in Appendix A giving a bi-invariant density $\tilde{h}_{\alpha,\tau}$ on $\mathbb{SL}(2)$. In particular $\tilde{h}_{\alpha_1,\tau_1} * h_{\alpha_2,\tau_2} \in \mathcal{F}_{\alpha_1+\alpha_2}(Q)$ for $\tau_1, \tau_2 > -1/4$, $\alpha_1, \alpha_2 > 1$ and suitable $Q > 0$.

We will not elaborate further on this topic, but we mention that motivated by our research and by many potential applications, the task of generalizing non-Gaussian distributions to hyperbolic spaces may lead to a new field of challenging research.

3. Main results. Let us begin with the definition of the Helgason–Fourier transform of the generalized derivative of the empirical distribution $f_Y^{(n)}(z) = \frac{1}{n} \sum_{j=1}^n \delta_{Y_j}(z)$ where Y_1, \dots, Y_n is a random sample in \mathbb{H}

$$(3.1) \quad \mathcal{H}f_Y^{(n)}(s, k) = \frac{1}{n} \sum_{j=1}^n (\operatorname{Im}(k(Y_j)))^{\bar{s}}.$$

Obviously

$$(3.2) \quad \mathbb{E}\mathcal{H}f_Y^{(n)}(s, k) = \mathcal{H}f_Y(s, k),$$

where “ \mathbb{E} ” denotes expectation. We estimate the Helgason transform of an $\mathbb{SO}(2)$ -invariant density as well by an $\mathbb{SO}(2)$ -invariant estimator

$$(3.3) \quad \mathcal{H}f_Y^{(n)}(s) := \mathcal{H}f_Y^{(n)}(s, \mathbf{I}) = \frac{1}{n} \sum_{j=1}^n \operatorname{Im}(Y_j)^{\bar{s}}$$

with the identity element $\mathbf{I} \in \mathbb{SO}(2)$.

From the Helgason–Fourier transform (3.1) we build an estimator by using (2.11) and the inverse Helgason–Fourier transformation (2.8) with a suitable cutoff $T > 0$

$$(3.4) \quad f_X^{(n,T)}(z) := \int_{|t|<T} \int_{u=0}^{u=2\pi} \frac{\mathcal{H}f_Y^n(1/2 + it, k_u)}{\mathcal{H}f_\varepsilon(1/2 + it)} (\operatorname{Im}(k_u(z)))^{1/2+it} d\tau$$

for the density f_X . This is well defined if $\mathcal{H}f_\varepsilon \neq 0$ is bounded from below on compact sets which is guaranteed under assumption (D.4). Even though we consider in this section the general case, we note in view of (3.3) and (2.10) that for the estimation of an $\mathbb{SO}(2)$ -invariant density f_X , we can use the simpler

$$f_X^{(n,T)}(e^{-r}i) := \frac{1}{4\pi} \int_{-T}^T \frac{\mathcal{H}f_Y^n(1/2 + it)}{\mathcal{H}f_\varepsilon(1/2 + it)} P_{-1/2+it}(\cosh r) t \tanh(\pi t) dt.$$

As the first main result we have:

THEOREM 3.1. *For f_X, f_Y and f_ε satisfying (D.1)–(D.3), and $\mathcal{H}f_\varepsilon \neq 0$ bounded from below on compact sets, there is a constant $C > 0$ not depending on T, α, Q and n such that*

$$\mathbb{E}\|f_X^{(n,T)} - f_X\|^2 \leq C \sup_{|t| \leq T} \left| \mathcal{H}f_\varepsilon \left(\frac{1}{2} + it \right) \right|^{-2} \frac{T^2}{n} + QT^{-2\alpha}$$

as $n \rightarrow \infty$.

If the corruption by error is smooth enough, or equivalently if the asymptotic rate of the decay of its Helgason–Fourier transform is suitable, the cutoff T can be adjusted appropriately to obtain the following rates.

THEOREM 3.2. *Suppose that f_X, f_Y and f_ε satisfy (D.1)–(D.4). Then by letting $T = (\frac{\gamma}{2} \log n - \frac{\eta\gamma}{2} \log(\log n))^{1/\beta}$ where $\eta \geq 2(\alpha + 1)/\beta$*

$$\mathbb{E}\|f_X^{(n,T)} - f_X\|^2 \leq Q \left(\frac{\gamma}{2} \log n \right)^{-2\alpha/\beta} (1 + o(1))$$

as $n \rightarrow \infty$ where α is from condition (D.3).

The optimal rate of a power of $\log n$ in case of error smoothness (D.4) is in agreement with Euclidean results. On the real line, condition (D.4) corresponds to supersmooth errors for which Fan [15] establishes the same type of rate. This rate has also been established by Butucea and Tsybakov [7] in case of additionally supersmooth signals. For a scenario corresponding to our setup on compact Lie groups, see [28] and more general on any compact manifold, see [27], where similar rates have been found.

The above results are minimax in the sense that the rate of convergence is matched by a corresponding lower bound. We have the following theorem.

THEOREM 3.3. *Suppose that f_X, f_Y and f_ε satisfy (D.1)–(D.4). Then for some constant $C > 0$, we have*

$$\inf \sup \mathbb{E}\|f^n - f_X\|^2 \geq C(\log n)^{-2\alpha/\beta}$$

as $n \rightarrow \infty$, where the infimum is taken over all estimators f^n and the supremum over all $f_X \in \mathcal{F}_\alpha(Q)$.

Recall the Gaussian density g_ρ on the real line with zero mean and variance $2\rho > 0$ can be characterized as yielding the solution of the heat equation

$$(\Delta - \partial_\rho)u = 0$$

with initial condition $u(z, 0) = f(z)$ by

$$(3.5) \quad u(z, \rho) = (g_\rho * f)(z).$$

Similarly on \mathbb{H} , the density g_ρ giving the solution of the heat equation by (3.5) is also called the Gaussian density for \mathbb{H} . Here, the Laplace–Beltrami operator Δ would be defined by (2.7), and the convolution in (3.5) would be defined as in (2.6). Using (2.11) for $\mathbb{S}\mathbb{O}(2)$ -invariant f and u it is easily seen that $\mathcal{H}g_\rho(s) \propto e^{\overline{s(s-1)}\rho}$. Consequently, in terms of assumption (D.4), the Gaussian density satisfies $\beta = 2$ and $\gamma = 1/\rho$. We have the following result.

COROLLARY 3.4. *For f_X and f_Y satisfying (D.1)–(D.3) consider corruption according to a Gaussian distribution $f_\varepsilon = g_\rho$. Then by letting $T^2 = \frac{1}{4\rho}[\log n - \eta \log(\log n)]$ where $\eta \geq 1 + \alpha$,*

$$\mathbb{E}\|f_X^{(n,T)} - f_X\|^2 \asymp (\log n)^{-\alpha}$$

as $n \rightarrow \infty$ gives the optimal rate of convergence.

4. Computations and simulations. In this section we elaborate on computational aspects, simulations and, in particular, discuss the Gaussian distribution on \mathbb{H} . We begin by first discussing methods for choosing the truncation parameter.

4.1. *Estimating truncation parameter.* A popular technique for data-driven choice of a truncation parameter is least squares cross-validation (see [13] or [45], Chapter 3.3). We will discuss how that technique can be adapted to our setting. For a given random sample Y_1, \dots, Y_n , an optimal cutoff $T = T_n^* > 0$ minimizes the mean integrated squared error

$$T_n^* = \arg \min_{T>0} \left\{ \mathbb{E} \left(\int_{\mathbb{H}} (f_X^{(n,T)}(z))^2 dz \right) - 2\mathbb{E} \left(\int_{\mathbb{H}} f_X(z) f_X^{(n,T)}(z) dz \right) \right\}.$$

Instead of deriving a minimizer of the above we content ourselves with minimizing a suitable estimator. Obviously, $\int_{\mathbb{H}} (f_X^{(n,T)}(z))^2 dz$ is an unbiased estimator of the first term. Let

$$f_X^{(n,T,l)} := \int_{-T}^T \int_0^{2\pi} \frac{1}{n-1} \sum_{j \neq l} \operatorname{Im}(k(Y_j))^{1/2-it} \operatorname{Im}(k(Y_l))^{1/2+it} \frac{d\tau}{\mathcal{H}f_\varepsilon(1/2+it)}$$

and therefore choose

$$T_n := \arg \min_{T>0} \left(\int_{\mathbb{H}} (f_X^{(n,T)}(z))^2 dz - \frac{2}{n} \sum_{l=1}^n f_X^{(n,T,l)} \right),$$

which is an estimate for an optimal $T = T_n^*$.

Alternatively, we can use the result of Corollary 3.2 and set

$$T = \left[\frac{\gamma}{2} \log n - \frac{\gamma}{2} \log(\log n)^\eta \right]^{1/\beta}.$$

We are aware of the fact that cross-validation in general suffers from too large variability and, of course, more involved parameter selection methods could be generalized here as well (see, e.g., [11, 12, 37, 40] and [42] among many others). However, we do not pursue this issue any further in this paper.

4.2. *Simulation of the Gaussian distribution.* For simulation we use the analog g_ρ of the Gaussian distribution on the upper half plane introduced above. Recall that by a more subtle argument (see [43], pages 153 and 155), the inverse transform is obtained in polar coordinates [for any $k \in \mathbb{S}\mathbb{O}(2)$]

$$\begin{aligned} g_\rho(k(e^{-r}i)) &= g_\rho(e^{-r}i) = \frac{1}{\sqrt{4\pi\rho^3}} \sqrt{2} e^{-\rho/4} \int_r^\infty \frac{b e^{-b^2/4\rho} db}{\sqrt{\cosh b - \cosh r}} \\ &=: \frac{\tilde{g}_\rho(r)}{2\pi \sinh r}; \end{aligned}$$

that is, for a ρ_X -Gaussian distributed $\mathbb{S}\mathbb{O}(2)$ -invariant random object X on \mathbb{H} and an $\mathbb{S}\mathbb{O}(2)$ -invariant subset $A \subset \mathbb{H}$,

$$\mathbb{P}\{X \in A\} = \int_{\{r \geq 0: e^{-r}i \in A \cap \mathbb{H}\}} \tilde{g}_{\rho_X}(r) dr$$

[see (A.2)]. Hence, in order to simulate X from an invariant Gaussian distribution we simulate $r_X \sim \tilde{g}_{\rho_X}$ on \mathbb{R} and u_X uniform on $[0, 2\pi)$; then

$$X = k_{u_X} \circ R_{r_X}(i) = k_{u_X}(e^{-r_X}i).$$

Note that $g_{\rho_X} \in \mathcal{F}_\alpha(Q)$ for all $\alpha > 0$ with suitable $Q = Q_\alpha > 0$. That is, f_X satisfies condition (D.3).

Similarly, in order to simulate ε from a bi-invariant ρ_ε -Gaussian distribution on $\mathbb{S}\mathbb{L}(2)$ we consider $r_\varepsilon \sim \tilde{g}_{\rho_\varepsilon}$ and $k_{u_\varepsilon}, k_{u'_\varepsilon}$ independent and uniform on $[0, 2\pi)$. Then

$$Y = k_{u_\varepsilon} \circ R_{r_\varepsilon} \circ k_{u'_\varepsilon}(X)$$

[see (2.4) and (A.3)].

According to Theorem 3.1, (3.1) and (3.4) we can then estimate the density f_X by

$$f_X^{(n,T)}(z) = \int_{|t| < T} \int_{u=0}^{u=2\pi} \frac{1/n \sum_{j=1}^n (\operatorname{Im}(k_u(Y_j)))^{1/2-it}}{e^{-(t^2+1/4)\rho_\varepsilon}} (\operatorname{Im}(k_u(z)))^{1/2+it} dt.$$

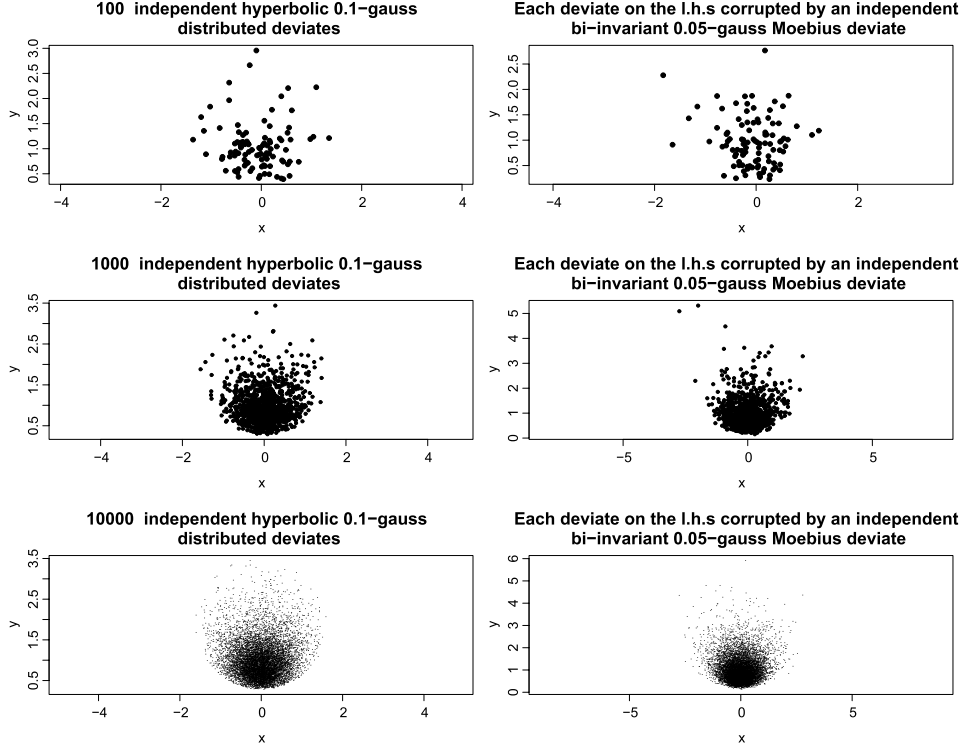


FIG. 2. Three simulated data samples of $n = 100$ (top row), $n = 1000$ (middle row) and $n = 10,000$ (bottom row) independent random data points on the upper half plane. Left row: original independent invariant ρ_X -Gaussian distributed data points, right row: transformed data points under independent n bi-invariant ρ_ε -Gaussian distributed $\mathbb{S}\mathbb{L}(2)$ transformations (right).

By $\mathbb{S}\mathbb{O}(2)$ -invariance it suffices to estimate for $z = e^{-r}i$ only, hence we estimate $\tilde{g}_{\rho_X}(r)$ by

$$\tilde{f}_X^{(n,T)}(r) := 2\pi \sinh r f_X^{(n,T)}(e^{-r}i)$$

with the integral simplified as in (2.10).

In the following simulation we consider an original distribution with $\rho_X = 0.1$ under a corrupting Möbius transformation distributed with $\rho_\varepsilon = 0.05$. From this we create three data sets with different sample sizes: $n = 100, 1000$ and $10,000$. Figure 2 shows the original X_1, \dots, X_n and the corrupted data $Y_1 = M_{\varepsilon_1}(X_1), \dots, Y_n = M_{\varepsilon_n}(X_n)$ in cartesian coordinates in the upper half plane. In Figure 3 we show the corresponding densities times hyperbolic area on $[0, \infty)$. Note that these are then densities in the usual sense; that is, their integrals with respect to Lebesgue measure on $[0, \infty)$ are 1. The density estimation by deconvolution has been obtained from the observed

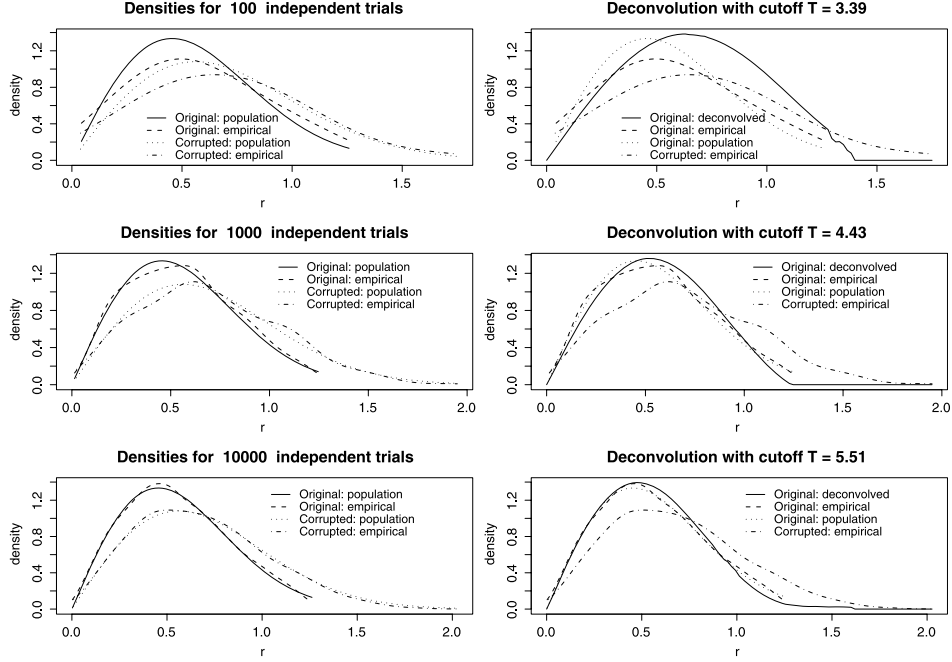


FIG. 3. *Left-hand side: population and empirical densities times hyperbolic area [corresponding to $\tilde{g}_{\rho_X}(r)$ and $\tilde{g}_{\rho_X+\rho_\varepsilon}(r)$] along the first polar coordinate r of the data depicted and described in Figure 2. Top row: $n = 100$, middle row: $n = 1000$ and bottom row: $n = 10,000$. Right-hand side: additionally the respective estimate times hyperbolic area: $\tilde{g}_X^{(n,T)}(r)$ of the original density by Möbius deconvolution. The corresponding optimal cutoff parameters $T = T_n$ have been estimated by least squares cross-validation as in Section 4.1.*

data Y_1, \dots, Y_n by the proposed method. For the deconvolution, since only the optimal rate

$$T \approx \left(\frac{1}{4\rho_\varepsilon} \log n \right)^{1/4} = \begin{cases} 2.19, & (n = 100), \\ 2.42, & (n = 1000), \\ 2.61, & (n = 10,000), \end{cases}$$

is guaranteed by Corollary 3.4, we have used the estimate via least squares cross-validation as proposed in Section 4.1.

4.3. *Simulation of the hyperbolic Laplace distribution.* Using formula (2.10) directly with (2.12) to simulate Laplace (α, τ) -deviates for Laplace distributed $\mathbb{S}\mathbb{L}(2)$ error corruption, we obtain results similar to the ones reported above. Due to the oscillation of the Legendre polynomials to be evaluated, however, the computational time is much longer. In analogy to Theorem 3.2 we have the upper bound $O(n^{-\alpha/(1+\alpha)})$ for the choice $T = n^{1/(2(\alpha+1))}$.

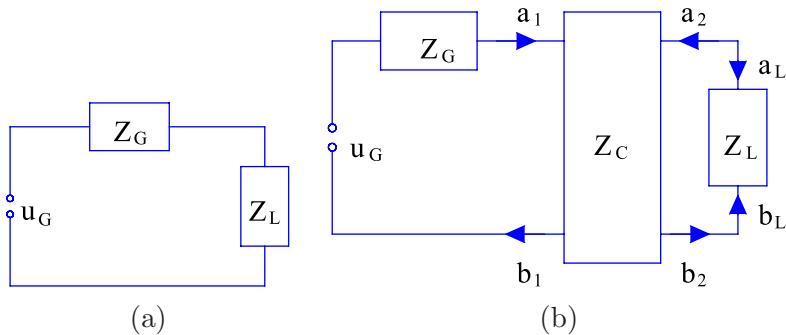


FIG. 4. *Basic circuit models for signal processing. Left: one-port, right: two-port. (a) Serial circuit with generated voltage u_G , generator impedance Z_G and load impedance Z_L ; (b) circuit of Figure 4(a) with a two-port inserted between generator and load, depicting input (a.) and output waves (b.) at the two-port and at load.*

5. Impedance density estimation in AC driven circuits. For the convenience of the reader, we begin this section with a review of classical electrical engineering theory specifically tailored to the application of hyperbolic statistics in mind. For the underlying engineering terminology we refer to standard textbooks such as [10]. More mathematical approaches are explained in [2, 20] and [43], Chapter 3. In the following we rephrase this problem in the language of statistics. We are then able to identify a typical problem as a novel inverse problem in hyperbolic space.

Here, general Möbius transformations appear with complex coefficients a , b , c , d in (2.1). Moreover, hyperbolic space materializes in the form of the upper half plane \mathbb{H} , the open unit disk $\mathbb{D} := \{w \in \mathbb{C} : |w| < 1\}$, and the open right half plane $-i\mathbb{H} := \{\zeta \in \mathbb{C} : \text{Re}(\zeta) > 0\}$. With the notation of (2.3), all are related to one another by Möbius transformations, the first is usually called the *Cayley transform*

$$(5.1) \quad \begin{aligned} w = \mathcal{C}(z) &:= \frac{z - i}{z + i}, & z &= i \frac{1 + w}{1 - w}, & i\zeta &= z, \\ w &= \frac{\zeta - 1}{\zeta + 1}, & \zeta &= \frac{1 + w}{1 - w}. \end{aligned}$$

5.1. Complex impedance in AC circuits. We begin our discussion with a *one-port*, a single load impedance serially inserted in a circuit of a voltage generator and its impedance [see Figure 4(a)]. Recall that voltages, currents and impedances in an alternating current (AC) circuit are modeled by complex numbers; otherwise, a loss of alternating real voltage $u : t \mapsto u_0 \cos(\omega t)$ over a load giving a phase shifted current $j : t \mapsto j_0 \cos(\omega t + \phi)$ would result into an awkward time dependent real resistance $u(t)/j(t)$. In complex

notation, the ratio of voltage $u(t) = u_0 e^{i\omega t}$ over current $j(t) = j_0 e^{i(\omega t + \phi)}$ is constant and called *impedance*

$$Z := \frac{u(t)}{j(t)} = \frac{u_0}{j_0} e^{i\phi} \in \mathbb{C}.$$

Its real part is called *resistance*, the imaginary part is the *reactance*. For example, under an AC-voltage $u_0 \cos(\omega)t$, a serial circuit of a resistor with direct current DC-resistance R and an ideal capacitor with capacitance C features an inverse impedance (called *admittance*) of $Z^{-1} = R^{-1} + i\omega C$. In fact, in realistic scenarios, the resistance is positive, thus $Z \in -i\mathbb{H}$, and the boundary (the imaginary axis) corresponds to ideal (lossless) impedances.

5.2. *Reflections and characteristic impedance.* We now assume that our circuit features a generator generating the *open circuit voltage* u_G with internal impedance Z_G and a load with impedance Z_L as depicted in Figure 4(a) with total impedance $Z = Z_G + Z_L$ according to Kirchhoff's circuit law.

Inspired by the wave model, voltage loss u_L over and current flow j_L along the load is considered to be the superimposition of an incoming (denoted by “+”) and a reflected wave (denoted by “−”) in such a way that each single wave satisfies Ohm's law with a common characteristic impedance Z_c . Since the reflected wave propagates into a direction opposite to the incoming wave, we have the *ansatz*

$$u_L = u_L^+ + u_L^- \quad \text{and} \quad j_L = j_L^+ - j_L^-$$

with Ohm's law

$$\frac{u_L^+}{j_L^+} = Z_c = \frac{u_L^-}{j_L^-} \quad \text{and} \quad \frac{u_L^+ + u_L^-}{j_L^+ - j_L^-} = Z_L.$$

The specific decomposition or equivalently the choice of Z_c is arbitrary in many applications, and it will be guided by imposing additional conditions. Usually Z_c is taken positive, or at least chosen such that the normalized impedances $\tilde{Z} := Z/Z_c$ will be again of positive real part, that is, $\tilde{Z} \in -i\mathbb{H}$. The analog for the right half plane of the Cayley transform, (5.1), yields then *reflection coefficient* of the load

$$(5.2) \quad \Gamma_L := \frac{u_L^-}{u_L^+} = \frac{j_L^-}{j_L^+} = \frac{Z_L - Z_c}{Z_L + Z_c} = \frac{\tilde{Z}_L - 1}{\tilde{Z}_L + 1} = \mathcal{C}(-i\tilde{Z}_L)$$

as an element of the unit-disk \mathbb{D} . Of course, there is no reflection if $Z_L = Z_c$.

5.3. *The chain matrix.* We are now in a position to investigate the generic scenario of signal transmission through a *two-port* [see Figure 4(b)]. Among others due to linearity of the Maxwell equations, voltages and currents ($j_1 = a_1, j_2 = a_2$) on either side of the two-port have a linear relationship governed by a so-called impedance matrix Z

$$Z \begin{pmatrix} j_1 \\ j_2 \end{pmatrix} = \begin{pmatrix} Z_{11} & Z_{12} \\ Z_{21} & Z_{22} \end{pmatrix} \begin{pmatrix} j_1 \\ j_2 \end{pmatrix} = \begin{pmatrix} u_1 \\ u_2 \end{pmatrix}.$$

For given circuit parameters, the coefficients of the impedance matrix can be easily computed. For example, $Z_{11} = \frac{u_1}{j_1}|_{j_2=0}$ is the well-known input-impedance (by inserting a load of infinite impedance the right-hand side becomes an open circuit with $j_2 = 0$). In most applications it turns out that Z is symmetric; the corresponding two-port is then called *reciprocal*.

One easily verifies that the *chain matrix* which is usually denoted by ch (the Russian letter “cha”) relating $(u_2, -j_2)$ with (u_1, j_1) is given by

$$\text{ch} \begin{pmatrix} u_2 \\ -j_2 \end{pmatrix} = \frac{1}{Z_{21}} \begin{pmatrix} Z_{11} & \det(Z) \\ 1 & Z_{22} \end{pmatrix} \begin{pmatrix} u_2 \\ -j_2 \end{pmatrix} = \begin{pmatrix} u_1 \\ j_1 \end{pmatrix}$$

[in contrast to the mathematical literature, the engineering literature tends to use a *transmission matrix* relating (u_2, j_2) with (u_1, j_1) instead, with reversed $j_2 = -a_2$ in Figure 4(b)]. An advantage of the chain matrix over the impedance matrix is that the former is well defined for the limit $Z_{21} \rightarrow \infty$, for example, for an ideal coil in series with the load.

Again, only using lossless (i.e., purely imaginary) impedances (such as ideal inductances, transformers and capacitors) guarantees that the corresponding chain matrix has real diagonal coefficients and imaginary coefficients elsewhere. Moreover, for cascaded two-ports (i.e., several two-ports in serial connection), the resulting chain matrix is just the product of the individual chain matrices. By linear algebraic decomposition of $\mathbb{S}\mathbb{L}(2, \mathbb{R})$ it can be shown that every lossless two-port of lumped elements can be modeled by cascading combinations of two-ports involving only inductances, transformers and capacitors (see [20], page 18). Note that $j_2 = a_2 = -a_L = -j_L$ in Figure 4(b). Hence ch defines a Möbius transformation relating load impedance with the input impedance of the two-port

$$M_{\text{ch}}(Z_L) = \frac{\text{ch}_{11}Z_L + \text{ch}_{12}}{\text{ch}_{21}Z_L + \text{ch}_{22}} = \frac{\text{ch}_{11}u_2 - \text{ch}_{12}j_2}{\text{ch}_{21}u_2 - \text{ch}_{22}j_2} = \frac{u_1}{j_1} = Z_1.$$

Here, $Z_1 = u_1/j_1$ is the impedance of the load $Z_L = -u_2/j_2$ as viewed through the two-port. As a consequence we make the following remark.

REMARK 5.1. Serial cascading of lossless two-ports is equivalent to the action of the Möbius group $\mathbb{S}\mathbb{L}(2, \mathbb{R})$ on the i -fold $iZ_L \in \mathbb{H}$ of load impedances Z_L .

We are thus led to the statistical inverse problem (cf. Problem 2.1).

PROBLEM 5.2. Estimate the load impedance Z_L when only the impedance $Z_{(1)}$ viewed through the two-port can be observed where $\varepsilon = \mathcal{I} \circ M_{\text{ch}} \circ \mathcal{I}^{-1} \in \mathbb{S}\mathbb{L}(2)$ is assumed to be of known distribution. Here, $\mathcal{I}: \mathbb{C} \rightarrow \mathbb{C}: z \rightarrow iz$ denotes the multiplication with i .

In conclusion we note that one may as well consider normalized impedances $\tilde{Z} = Z/Z_c$ or equivalently reflection coefficients, (5.2). Then the mapping for the normalized impedances goes as follows:

$$\frac{Z_1}{Z_c} = \frac{\text{ch}_{11}Z_L/Z_c + \text{ch}_{12}/Z_c}{Z_c\text{ch}_{12}Z_L/Z_c + \text{ch}_{22}}.$$

5.4. *Estimating resistances seen through electrolyte capacitors.* It is well known that over the duration of years properties of electronic equipment change due to wear-out effects of various elements. In particular, electrolyte capacitors have a tendency to loose capacitance. In effect, older electronic devices deviate from original calibration and may feature undesired side-effects; for example, field strengths of transmitters may grow stronger than tolerated.

In an application of our method we consider a series of $n = 150$ measurements of random resistors of 15Ω provided with an accuracy of 10 percent by the manufacturer (they range from 13.5Ω to 17.7Ω) viewed through 30 random capacitors at 1 kHz taken at the Department of Electrical Engineering, University of Applied Sciences, Fulda, Germany. These originally identical lossy $22 \mu\text{F}$ capacitors have been collected from over ten year old electronic gear. For the impedance measurements the LCR-Bridge ‘‘HM8118’’ has been used that comes with an accuracy of 0.3% guaranteed by its producer HAMEG. We model the i -fold of the impedance Z of these capacitors with a hyperbolic Gaussian-distribution at unit impedance, that is, $Zi = Z_c M_{\rho_\varepsilon}(i)$ with a suitable characteristic impedance Z_c and a random hyperbolic Gaussian ρ -distributed Möbius transformation M_{ρ_ε} . Measurement of the capacitors gives $\rho_\varepsilon \approx 0.0004$ corresponding to a spread of roughly 4.8%. Our goal lies in the reconstruction of the one-dimensional resistances R solely from the observations

$$W = \frac{1}{1/R + 1/Z} = \frac{ZR}{Z + R}$$

and the known dispersion ρ_ε of the corruption as posed in Problem 5.2. To this end we apply Möbius deconvolution to the model

$$\frac{W}{W_c} i = M_\varepsilon \left(\frac{R}{R_c} i \right)$$

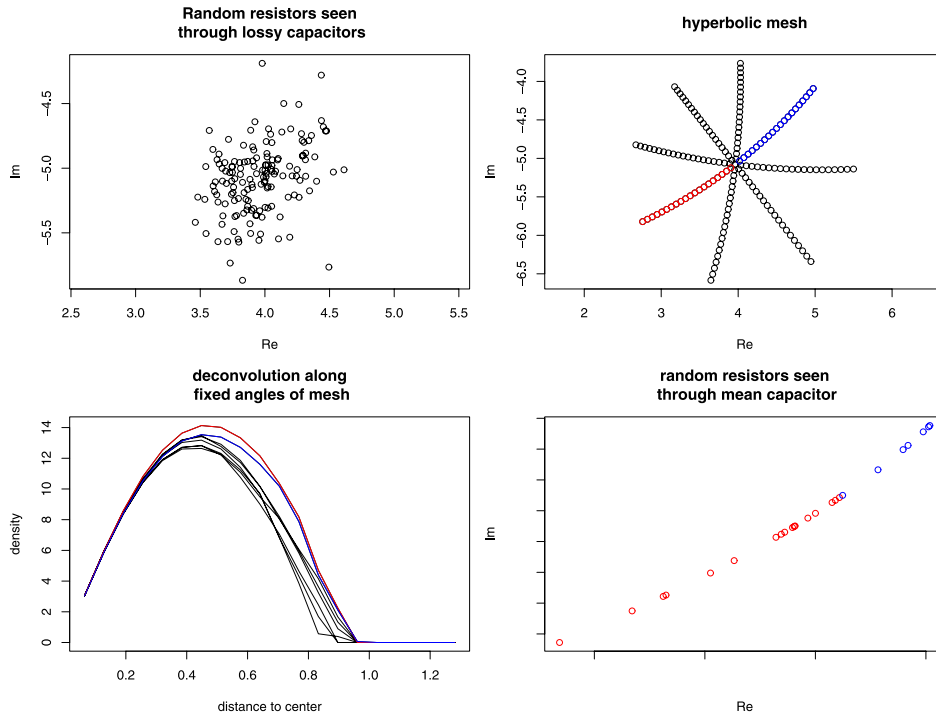


FIG. 5. *Random resistors seen through random capacitors. Left top: original measurements. Right top: hyperbolic polar mesh points at which the Möbius deconvolution was computed. The bottom left image depicts the deconvolved densities times hyperbolic measure along fixed angles. The red and blue line goes along the red and blue mesh points. For verification, the one-dimensional distribution of the resistors seen through the single mean capacitor is depicted in the bottom right image.*

with suitable characteristic impedances W_c and R_c . For this application the Euclidean means have been chosen as characteristic impedances. Alternatively, a better approach may be to use hyperbolic intrinsic means (see [3] and [4]). Figure 5 shows the observations W in the left top corner. Möbius deconvolution is computed along the hyperbolic polar mesh-points depicted in the right top corner (Figure 5). Below in the bottom left corner the deconvolved densities along fixed angles of the mesh are depicted. The angle depicted in red shows highest density followed by the angle depicted in blue. The location of the two dominating directions depicted with the same colors in the right top corner (Figure 5) is in high agreement with the location of the impedances of the resistors seen through the mean capacitor depicted in the bottom right image of Figure 5. Indeed, one can say that with the few measurements available, we were able to reconstruct the nature of the unobserved elements, namely resistors with impedances distributed along a one-dimensional subset in the complex half plane.

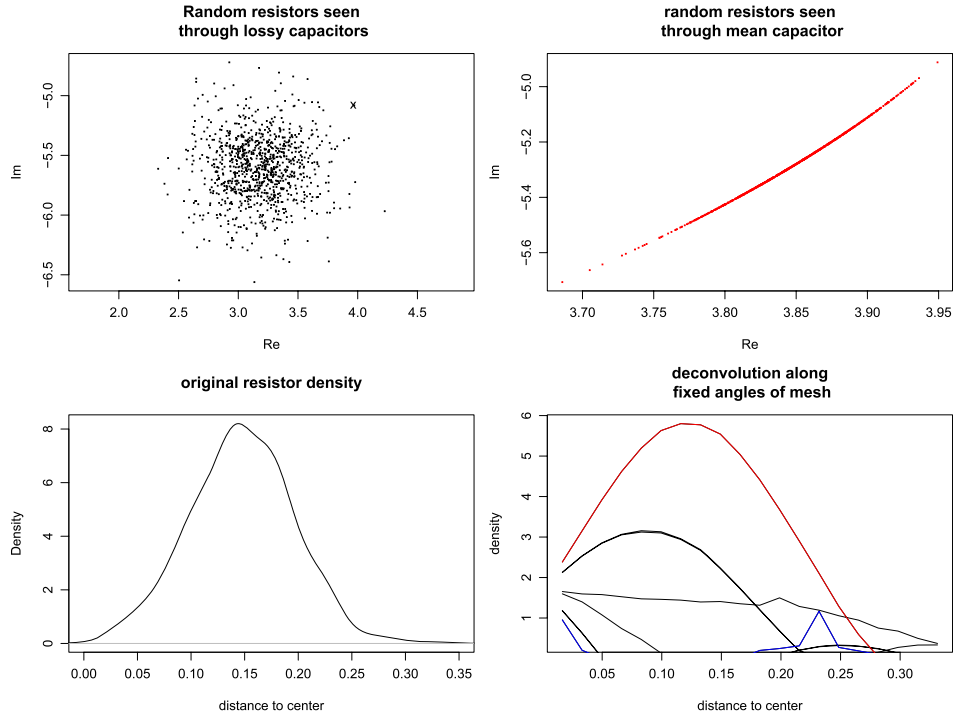


FIG. 6. Simulation of $n = 1000$ random resistors seen through n random capacitors. Top left: observed impedances, characteristic impedance denoted by “ x .” Top right: unobserved underlying normalized resistors seen through unobserved mean capacitor. Bottom left: radial density times hyperbolic measure of nonobserved resistors. Bottom right: deconvolved densities times hyperbolic measure along fixed angles of mesh in Figure 5.

In Figure 6 the above scenario is more prominently reenacted in a simulation of $n = 1000$ measurements using $R_c = \min(R)$ and W_c from the preceding example (depicted by “ x ”). We show observed measurements and unobserved capacitors in the top row as well as original density and the deconvolved densities along respective angles as in Figure 5 in the bottom row. Obviously the distribution of the unobserved resistors is quite reasonably recovered along the grid.

APPENDIX A: POLAR COORDINATES AND CONVOLUTION

In this appendix we focus on the right and left action (they are different due to noncommutativity) of the special orthogonal group $\mathbb{S}\mathbb{O}(2)$ on $\mathbb{S}\mathbb{L}(2)$ giving rise to polar coordinates and to \mathbb{H} viewed as the quotient with respect to one of the actions. In fact, the action of $\mathbb{S}\mathbb{L}(2)$ on \mathbb{H} can be naturally viewed in polar coordinates (cf. Figure 7) of which we will make extensive use in the proof of Theorem 3.3 in Appendix B.3.

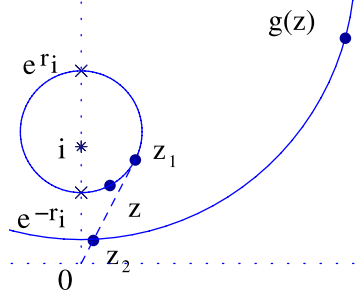


FIG. 7. The polar coordinates (r, u) of $z \in \mathbb{H}$ are obtained from the unique circle hyperbolically centered at i (star) containing z ; that is, this circle is symmetric to the imaginary axis and intersects it at points of form $e^{-r}i$ and e^ri (x-crosses). Rotating z by the hyperbolic angle $-u$ along this circle, the lower point $e^{-r}i$ is obtained. The polar coordinates (u_2, R, u_1) of $g \in \mathbb{S}\mathbb{L}(2)$ rotate z by the hyperbolic angle u_1 along the above circle to obtain z_1 , rescale z_1 by e^{-R} to obtain $z_2 = e^{-R}z_1$ and subsequently rotate z_2 by the hyperbolic angle u_2 along the unique hyperbolic circle through z_2 hyperbolically centered at i yielding $g(z)$.

In contrast to a metric on a manifold in the usual topological sense, a *Riemannian metric* is a metric in every tangent space, that varies smoothly with the offset of the tangent space. Thereby, every Riemannian metric defines a metric on the manifold in the usual sense and a unique volume element, called the *Riemannian volume*, giving rise to a unique measure on the manifold. For more details we refer to Lee [31], Chapter 3.

If the Riemannian metric on $\mathbb{S}\mathbb{L}(2)$ underlying the Haar measure dg is chosen such that the natural Riemannian quotient metric on \mathbb{H} yields the hyperbolic measure dz on \mathbb{H} , then we are able to lift densities on the bottom space \mathbb{H} to the top space $\mathbb{S}\mathbb{L}(2)$ to obtain (A.4) yielding (2.6).

Let us begin with the observation that the hyperbolic measure (2.5) is the Riemannian volume element of the extension of the standard Euclidean metric in the tangent space of \mathbb{H} at $z = i$ in a left-invariant way under the action of $\mathbb{S}\mathbb{L}(2)$ on \mathbb{H} . Similarly, we equip $\mathbb{S}\mathbb{L}(2)$ with the Riemannian metric obtained from the left $\mathbb{S}\mathbb{L}(2)$ -invariant extension of the standard Euclidean metric in the tangent space of the unit matrix $\mathbf{I} \in \mathbb{S}\mathbb{L}(2)$. We denote the corresponding Riemannian volume element which defines a left-invariant Haar measure by dg . According to [43], Exercise 19, page 149, it is also right invariant, that is,

$$\int_{\mathbb{S}\mathbb{L}(2)} f(agb) dg = \int_{\mathbb{S}\mathbb{L}(2)} f(g) dg \quad \forall a, b \in \mathbb{S}\mathbb{L}(2), f \in L^1(\mathbb{S}\mathbb{L}(2), dg).$$

As mentioned before, for arbitrary $z, z' \in \mathbb{H}$ there exists a $g \in \mathbb{S}\mathbb{L}(2)$ such that $z' = M_g(z)$. Given one such g , any other $g' \in \mathbb{S}\mathbb{L}(2)$ satisfies $M_{g'}(z) = z'$ if, and only if, $g^{-1}g' \in \mathbb{S}\mathbb{O}(2)$. In particular, $M_g(i) = i$ if, and only if, $g \in \mathbb{S}\mathbb{O}(2)$.

This entails that the following mapping of the quotient space $\mathbb{S}\mathbb{L}(2)/\mathbb{S}\mathbb{O}(2)$ due to the right action of $\mathbb{S}\mathbb{O}(2)$ is well defined and bijective

$$(A.1) \quad \left. \begin{array}{l} \mathbb{S}\mathbb{L}(2)/\mathbb{S}\mathbb{O}(2) \rightarrow \mathbb{H} \\ g\mathbb{S}\mathbb{O}(2) \mapsto M_g(i) \end{array} \right\}.$$

Since the mapping preserves the action of $\mathbb{S}\mathbb{L}(2)$, the natural Riemannian quotient metric of $\mathbb{S}\mathbb{L}(2)/\mathbb{S}\mathbb{O}(2)$ is isometric with the the hyperbolic metric of \mathbb{H} .

Next, consider the left action of $\mathbb{S}\mathbb{O}(2)$ on $\mathbb{S}\mathbb{L}(2)$. This projects to a left-action on \mathbb{H} giving rise to polar coordinates $u \in [0, 2\pi)$, called the *hyperbolic angle* and $r > 0$ (cf. Figure 7) of

$$z = M_{k_u} \circ M_{R_r}(i) \quad \text{with } k_u = \begin{pmatrix} \cos u & \sin u \\ -\sin u & \cos u \end{pmatrix}, R_r = \begin{pmatrix} e^{-r/2} & 0 \\ 0 & e^{r/2} \end{pmatrix}.$$

For ease of notation, for the entire paper we identify M_{k_u} with k_u and M_{R_r} with R_r , respectively, such that $k_u \circ R_r(i) = k_u(e^{-r}i)$. Since for every $z \in \mathbb{H} \setminus \{i\}$ we have that $k_\phi(z) = z$ if, and only if $\phi \equiv 0 \pmod{\pi}$, polar coordinates cover the hyperbolic plane twice. As a consequence, $z \in \mathbb{H}$ has polar coordinates with $r \geq 0$ uniquely determined and u unique modulo π if $r > 0$. Thus, the hyperbolic area element (2.5) transforms to

$$(A.2) \quad dz = \sinh(r) dr du.$$

Polar coordinates can also be defined on $\mathbb{S}\mathbb{L}(2)$: every element $g \in \mathbb{S}\mathbb{L}(2)$ has a decomposition

$$(A.3) \quad g = k_u R_r k_{u'}, \quad r \in [0, \infty), u, u' \in [0, 2\pi),$$

with uniquely determined $r \geq 0$; if $r > 0$ then u and u' are also uniquely determined modulo π (in fact, one of the two is unique modulo 2π). In view of the isometry (A.1), this gives our choice of Haar measure in polar coordinates

$$dg = \sinh(r) dr du du'.$$

If g, g' are independent random elements in $\mathbb{S}\mathbb{L}(2)$ with densities f_1, f_2 continuous with respect to Haar measure, we have for the probability that the product is contained in a measurable subset $A \subset \mathbb{S}\mathbb{L}(2)$ by left-invariance of the measure that $\mathbb{P}(gg' \in A) = \int_A (f_1 * f_2)(a) da$ with the convolution of f_1 and f_2 given by

$$(f_1 * f_2)(a) := \int_{\mathbb{S}\mathbb{L}(2)} f_1(g) f_2(g^{-1}a) dg.$$

In general, convolutions over noncommutative groups are noncommutative.

Suppose now that Z is a random quantity on \mathbb{H} with density f_2 continuous with respect to the hyperbolic measure. Using polar coordinates, this

density lifts to a right $\mathrm{SO}(2)$ -invariant density \tilde{f}_2 on $\mathrm{SL}(2)$ $\tilde{f}_2(k_u R_r k'_u) := f_2(k_u R_r(i))$. Hence, convolutions of a density f_1 on $\mathrm{SL}(2)$ with a density f_2 on \mathbb{H} can be well defined by lifting to a right $\mathrm{SO}(2)$ -invariant density on $\mathrm{SL}(2)$

$$(A.4) \quad (f_1 * f_2)(z) := \int_{\mathrm{SL}(2)} f_1(g) \tilde{f}_2(g^{-1}a) dg$$

with any $a \in \mathrm{SL}(2)$ giving $M_a(i) = z$. This convolution is commutative if either f_1 is bi-invariant or if f_2 is $\mathrm{SO}(2)$ -invariant.

APPENDIX B: PROOFS

B.1. Upper bound: Proof of Theorem 3.1. In order to measure the performance of $f_X^{(n,T)}$ we consider the mean integrated squared error

$$\mathbb{E} \|f_X - f_X^{(n,T)}\|^2 = \mathbb{E} \|f_X - \mathbb{E} f_X^{(n,T)}\|^2 + \|\mathbb{E} f_X^{(n,T)} - f_X\|^2$$

with the usual variance-bias decomposition. The assertion of Theorem 3.1 then follows from the following more detailed lemma.

LEMMA B.1. *For f_X, f_Y and f_ε satisfying (D.1) and (D.2), and $\mathcal{H}f_\varepsilon$ bounded from below on compact sets, there is a constant $C > 0$ independent of T and n such that*

$$\mathbb{E} \|f_X - \mathbb{E} f_X^{(n,T)}\|^2 \leq \frac{C}{\inf_{|t| < T} |\mathcal{H}f_\varepsilon(1/2 + it)|^2} \frac{T^2}{n}.$$

If, additionally, f_X satisfies (D.3), then

$$\|\mathbb{E} f_X^{(n,T)} - f_X\|^2 \leq QT^{-2\alpha}.$$

PROOF. We first note that by (2.8), definition (3.4), since the right-hand side is in $L^2(\mathbb{H}, dz)$,

$$\mathcal{H}f_X^{(n,T)}\left(\frac{1}{2} + it, k\right) = \frac{\mathcal{H}f_Y^n(1/2 + it, k)}{\mathcal{H}f_\varepsilon(1/2 + it, k)} \mathbb{I}_{(-T, T)}(t).$$

Here \mathbb{I} denotes the *indicator function*. Hence by the Fubini–Tonelli theorem, (3.4), (3.2), (2.8) and (2.11)

$$\begin{aligned} & \mathcal{H}(\mathbb{E} f_X^{(n,T)})\left(\frac{1}{2} + it, k\right) \\ &= \mathcal{H}\left(z \rightarrow \int_{|t'| < T} \int_{u'=0}^{u'=2\pi} \frac{\mathbb{E} \mathcal{H}f_Y^n(1/2 + it', k_{u'})}{\mathcal{H}f_\varepsilon(1/2 + it')} \right) \end{aligned}$$

$$(B.1) \quad \begin{aligned} & \times (\operatorname{Im}(k_{u'}(z)))^{1/2+it'} d\tau' \left(\frac{1}{2} + it, k \right) \\ & = \mathcal{H}f_X \left(\frac{1}{2} + it, k \right) \mathbb{I}_{(-T, T)}(t). \end{aligned}$$

Deduce from (3.1),

$$(B.2) \quad \begin{aligned} & \mathbb{E} \left| \mathcal{H}f_Y^{(n)} \left(\frac{1}{2} + it, k \right) \right|^2 \\ & = \left| \mathcal{H}f_Y \left(\frac{1}{2} + it, k \right) \right|^2 + \frac{\operatorname{Im}(\mathbb{E}k(Y)) - |\mathcal{H}f_Y(1/2 + it, k)|^2}{n}. \end{aligned}$$

In addition, $\operatorname{Im}(\mathbb{E}k(Y)) = \mathcal{H}f_Y(1, k)$ implies that

$$(B.3) \quad \int_0^{2\pi} |\operatorname{Im}(\mathbb{E}k_u(Y))| du = \int_0^{2\pi} |\mathcal{H}f_Y(1, k_u)| du \leq C$$

with a suitable constant $C > 0$, since $\mathcal{H}f_Y$ is analytic. Thus, using the Plancherel identity (2.9), (2.11), the Fubini–Tonelli theorem, (3.2), (B.1), (B.2) and (B.3) [by hypothesis (D.1) and (2.9), $\|f_Y\|^2 = \|\mathcal{H}f_Y\|^2 < \infty$], we have indeed for the variance

$$\begin{aligned} & \mathbb{E} \int_{\mathbb{H}} |f_X^{(n, T)} - \mathbb{E}f_X^{(n, T)}|^2 dz \\ & = \int_{t < |T|} \int_{u \in [0, 2\pi)} \frac{\mathbb{E} |\mathcal{H}f_Y^{(n)} - \mathcal{H}f_Y|^2}{|\mathcal{H}f_\varepsilon|^2} d\tau \\ & = \frac{1}{n} \frac{1}{8\pi^2} \int_{t < |T|} \int_{u \in [0, 2\pi)} \frac{\operatorname{Im}(\mathbb{E}k_u(Y)) - |\mathcal{H}f_Y(1/2 + it)|^2}{|\mathcal{H}f_\varepsilon(1/2 + it)|^2} t \tanh(\pi t) dt du \\ & \leq \frac{C}{\inf_{|t| < T} |\mathcal{H}f_\varepsilon(1/2 + it)|^2} \frac{T^2}{n} \end{aligned}$$

with a constant $C > 0$ involving neither n nor T .

In the next step we similarly estimate the squared bias under the additional assumption (D.3) using also (2.9) and (B.1)

$$\begin{aligned} & \int_{\mathbb{H}} |\mathbb{E}f_X^{(n, T)} - f_X|^2 dz \\ & = \int_{|t| \geq T} \int_{u \in [0, 2\pi)} |\mathcal{H}f_X|^2 d\tau \\ & = \frac{1}{8\pi^2} \int_{|t| \geq T} \int_{u=0}^{u=2\pi} \left| \left(\frac{1}{2} + it \right) \left(-\frac{1}{2} + it \right) \right|^{-\alpha} \left| \left(\frac{1}{2} + it \right) \left(-\frac{1}{2} + it \right) \right|^\alpha \end{aligned}$$

$$\begin{aligned} & \times \left| \mathcal{H}f_X \left(\frac{1}{2} + it, k_u \right) \right|^2 t \tanh(\pi t) dt du \\ & \leq QT^{-2\alpha}. \end{aligned} \quad \square$$

B.2. Optimal rate: Proof of Theorem 3.2. If f_ε satisfies (D.4) we have the upper bound

$$(B.4) \quad \log C + \log C_1 + 2 \log T - \log n + \frac{2}{\gamma} T^\beta \left(1 + \frac{1}{4T^2} \right)^{\beta/2}$$

for the logarithm of the variance term (cf. Lemma B.1). A sufficient condition for convergence of the variance term while $T = T(n) \rightarrow \infty$, is that (B.4) tends to $-\infty$. Hence, T is of form

$$T(n) = \left(\frac{\gamma}{2} \log n - \frac{\gamma}{2} A(n) \right)^{1/\beta}$$

with $A(n) \rightarrow +\infty$ at a rate lower than that of $\log n$. A short computation gives the rate

$$\frac{2}{\beta} \log(\log n) - A(n)$$

for (B.4). In case of optimality this rate must be larger or equal to the logarithmic rate of the upper bound of the bias term in Lemma B.1 which is then

$$-\frac{2\alpha}{\beta} \log(\log n).$$

In consequence the rate of $A(n)$ is $\eta \log(\log n)$ with $\eta \geq 2(1+\alpha)/\beta$ as asserted by Theorem 3.2.

B.3. Lower bound properties: Proof of Theorem 3.3. Recall the decomposition in polar coordinates from Appendix A (cf. Figure 7). The general idea of proof goes as follows. Define the *dilation* of H by

$$(B.5) \quad H^\delta(k(e^{-r}i)) := H(k(e^{-\delta r}i)) \frac{\sinh(\delta r)}{\sinh r} P_{-1/2}(\cosh(\delta r)).$$

For arbitrary $\mathbb{S}\mathbb{O}(2)$ -invariant H and $\delta > 0$, H^δ is obviously also $\mathbb{S}\mathbb{O}(2)$ -invariant

To derive a lower bound for estimating f_X in L^2 norm, we follow a classical scheme which has been condensed in [15], pages 1261 and 1262 (cf. also [18], pages 1555 and 1556). The adaption of this scheme to the Poincaré plane, however, is not at all obvious and will be the subject of the following sections.

After some elaborate preparation in the following two sections we take a pair $f_0 \in \mathcal{F}_\alpha(Q)$, $f_n \in \mathcal{F}_\alpha(Q)$, for which

$$f_n = f_0 + C_H \delta^{-\alpha} H^\delta,$$

where $\delta = \delta_n$ (cf. Sections B.3.3 and B.3.4 below). Then, in Section B.3.5 we show that δ can be chosen such that

$$(B.6) \quad \chi^2(f_\varepsilon * f_0, f_\varepsilon * f_n) := \int_0^\infty (f_\varepsilon * f_0 - f_\varepsilon * f_n)^2 (f_\varepsilon * f_0)^{-1} dz \leq \frac{C}{n}.$$

In consequence by (3.3) of [15], there is $d_1 > 0$ such that for any estimator f^n of f_X ,

$$(B.7) \quad \sup_{f_X \in \{f_0, f_n\}} \mathbb{P}_f \{ \|f^n - f_X\|_2 > \|f_0 - f_n\|_2 / 2 \} > d_1,$$

which gives with (3.4) of [15] a lower bound

$$\sup_{f_X \in \mathcal{F}_\alpha(Q)} E \|f^n - f_X\|_2^2 \geq \frac{d_1}{4} \|f_0 - f_n\|_2 \asymp \delta^{-\alpha} \|H^\delta\|_2.$$

The choice of δ in (B.17) at the end of Section B.3.5 in conjunction with $\|H^\delta\|^2 \asymp \|H\|^2$ from Lemma B.5 then yields the rate

$$\delta^{-\alpha} \|H^\delta\|^2 \asymp (\log n)^{-2\alpha/\beta}$$

asserted by Theorem 3.3.

B.3.1. Convolution equation in polar coordinates.

LEMMA B.2. *Suppose f is bi-invariant and h is $\mathbb{SO}(2)$ -invariant. Write $z = k_u R_r(i)$, $g = k_\alpha R_s k_\beta \in \mathbb{SL}(2)$ and $dg = \sinh s d\alpha ds d\beta$. Then,*

$$(f * h)(z) = 2\pi \int_{\phi=0}^{2\pi} \int_{s=0}^{\infty} f(e^{-s}i) h(e^s k_{-\phi}(e^{-r}i)) \sinh s d\phi ds.$$

PROOF. Since $k_{-\alpha} k_u = k_{u-\alpha}$ observe that

$$\begin{aligned} (f * h)(z) &= \int_{\mathbb{SL}(2)} f(g) h(g^{-1}z) dg \\ &= \int \int_{\alpha, \beta \in [0, 2\pi)} \int_{s=0}^{s=\infty} f(k_\alpha R_s k_\beta) h(k_{-\beta} R_{-s} k_{-\alpha} k_u R_r(i)) \\ &\quad \times \sinh s d\alpha ds d\beta \\ &= 2\pi \int_{\phi=0}^{2\pi} \int_{s=0}^{\infty} f(e^{-s}i) h(R_{-s} k_{-\phi} R_r(i)) \sinh s d\phi ds. \quad \square \end{aligned}$$

LEMMA B.3. Define $\eta(r, s, \phi)$ and $R(r, s, \phi)$ by $k_{\eta(r, s, \phi)} e^{-R(r, s, \phi)} i = e^s k_{-\phi} \times e^{-r} i$, where $0 \leq \eta(r, s, \phi) < 2\pi$ and $R(r, s, \phi) \geq 0$. Suppose $\phi \in [0, 2\pi)$ and $r, s \geq 0$. Then,

$$|r - s| \leq R(r, s, \phi) \leq r + s.$$

PROOF. Let $\psi = 2\phi$. From [43], page 125, we take

$$k_{-\phi} e^{-r} i = \frac{-\sin \psi \sinh r + i}{\cos \psi \sinh r + \cosh r}.$$

Let $k_{\eta(r, s, \phi)} e^{-R(r, s, \phi)} i = x + iy$. Then using [43], page 150,

$$\begin{aligned} \cosh(R(r, s, \phi)) &= \frac{1}{2} \frac{1 + x^2 + y^2}{y} \\ &= \frac{1}{2} \left(e^{-s} (\cos \psi \sinh r + \cosh r) + e^s \frac{\sin^2 \psi \sinh^2 r + 1}{\cos \psi \sinh r + \cosh r} \right). \end{aligned}$$

Set $t = \cos \psi$. Since

$$\begin{aligned} \frac{\sin^2 \psi \sinh^2 r + 1}{\cos \psi \sinh r + \cosh r} &= \frac{(1 - t^2) \sinh^2 r + 1}{t \sinh r + \cosh r} \\ &= \cosh r - t \sinh r, \end{aligned}$$

we have

$$\begin{aligned} \cosh(R(r, s, \phi)) &= \frac{1}{2} \{ e^{-s} (\cosh r + t \sinh r) + e^s (\cosh r - t \sinh r) \} \\ &= -t \sinh r \sinh s + \cosh r \cosh s. \end{aligned}$$

Since $-1 \leq t \leq 1$, $\cosh(R(r, s, \phi))$ has the maximum $\cosh(r + s)$ at $t = -1$ and the minimum $\cosh(r - s)$ at $t = 1$. Suppose that $\cosh a \leq \cosh b$ with $b \geq 0$. This implies that $b \geq |a|$ since

$$\begin{cases} b \geq a, & \text{if } a \geq 0, \\ b \geq -a, & \text{if } a < 0. \end{cases}$$

The desired result follows from this and the assumption $R(r, s, \phi) \geq 0$. \square

The following lemma is an immediate consequence of Lemma B.3.

LEMMA B.4. Suppose H is $\mathbb{S}\mathbb{O}(2)$ -invariant and $H(e^{-r} i)$ is monotonically decreasing in r . Then,

$$H(e^s k_{-\phi} e^{-r} i) \leq H(e^{-|r-s|} i) \quad \text{for } s \geq 0, \phi \in [0, 2\pi), r \geq 0.$$

B.3.2. *Dilation.*LEMMA B.5. *Suppose*

$$(B.8) \quad \mathcal{H}H\left(\frac{1}{2} + it\right) = 0 \quad \text{for } t \notin \left[\frac{1}{2}, 1\right].$$

Then for $\delta \rightarrow \infty$,

$$(B.9) \quad \begin{aligned} \mathcal{H}H^\delta\left(\frac{1}{2} + it\right) &\asymp \frac{1}{\delta} \mathcal{H}H\left(\frac{1}{2} + i\frac{t}{\delta}\right), \\ \|H^\delta\|^2 &\asymp \|H\|^2, \\ \|\Delta^{\alpha/2} H^\delta\|_2 &\asymp \delta^{\alpha/2} \|\Delta^\alpha H\|_2 \end{aligned}$$

and for f_ε satisfying (D.4) with $\gamma = 1$, with a constant $C > 0$,

$$\int |f_\varepsilon * H^\delta|^2 \leq C e^{-2(\delta/2)^{2\beta}}.$$

PROOF. Let's start with an alternate representation of the Legendre function from [43], page 158, and a specific derivative

$$\begin{aligned} P_{-1/2+it}(\cosh r) &= \frac{\sqrt{2}}{\pi} \int_0^r \frac{\cos(tu) du}{\sqrt{\cosh r - \cosh u}}, \\ A(\cosh r) &:= -\frac{\partial^2}{(\partial t)^2} \Big|_{t=0} P_{-1/2+it}(\cosh r) \\ &= \frac{\sqrt{2}}{\pi} \int_0^r \frac{u^2 du}{\sqrt{\cosh r - \cosh u}}. \end{aligned}$$

In the next step we make use of [43], Exercise 28(b), page 158. For fixed $t, \kappa > 0$, and large δ , that is, $r = \kappa/\delta \rightarrow 0$

$$\begin{aligned} P_{-1/2+it}\left(\cosh \frac{\kappa}{\delta}\right) &\asymp J_0\left(\frac{t\kappa}{\delta}\right) \\ &= \sum_{j=0}^{\infty} \frac{(-1)^j}{(j!)^2} \left(\frac{t\kappa}{2\delta}\right)^{2j} \\ &= 1 - \frac{1}{4} \left(\frac{t}{\delta}\right)^2 \kappa^2 + \dots \end{aligned}$$

Similarly,

$$P_{-1/2+it/\delta}(\cosh \kappa) = P_{-1/2}(\cosh \kappa) - \frac{A(\kappa)}{2} \left(\frac{t}{\delta}\right)^2 + \dots$$

Then with the two above developments,

$$\begin{aligned}\mathcal{H}H^\delta\left(\frac{1}{2}+it\right) &= \frac{2\pi}{\delta} \int_0^\infty H(e^{-\kappa}i)P_{-1/2}(\cosh \kappa)\left(1+O\left(\frac{1}{\delta^2}\right)\right)\sinh(\kappa) d\kappa \\ &\asymp \frac{2\pi}{\delta} \int_0^\infty H(e^{-\kappa}i)P_{-1/2+it/\delta}(\cosh \kappa)\sinh(\kappa) d\kappa \\ &= \frac{1}{\delta}\mathcal{H}H\left(\frac{1}{2}+i\frac{t}{\delta}\right).\end{aligned}$$

Moreover since $\mathcal{H}H(\frac{1}{2}+iu) = 0$ for $u \in (0, \frac{1}{2})$,

$$\begin{aligned}\|\mathcal{H}H^\delta\|_2^2 &\asymp \frac{1}{4\pi} \int_0^\infty \frac{1}{\delta^2} \left| \mathcal{H}H\left(\frac{1}{2}+i\frac{t}{\delta}\right) \right|^2 t \tanh(\pi t) dt \\ &= \frac{1}{4\pi} \int_0^\infty \left| \mathcal{H}H\left(\frac{1}{2}+iu\right) \right|^2 \frac{\tanh(\pi\delta u)}{\tanh(\pi u)} u \tanh(\pi u) du \\ &\asymp \|H\|_2^2\end{aligned}$$

and taking additionally into account that δ is large

$$\begin{aligned}\|\Delta^{\alpha/2}H^\delta\|_2^2 &\asymp \frac{1}{4\pi} \int_0^\infty (t^2+1/4)^\alpha \frac{1}{\delta^2} \left| \mathcal{H}H\left(\frac{1}{2}+i\frac{t}{\delta}\right) \right|^2 t \tanh(\pi t) dt \\ &\leq \delta^{2\alpha} \frac{1}{4\pi} \int_0^\infty \left(u^2+\frac{1}{4}\right)^\alpha \left| \mathcal{H}H\left(\frac{1}{2}+iu\right) \right|^2 \frac{\tanh(\pi\delta u)}{\tanh(\pi u)} u \tanh(\pi u) du \\ &\leq C\delta^{2\alpha}\|\Delta^{\alpha/2}H\|_2^2.\end{aligned}$$

Since by hypothesis

$$|\mathcal{H}f_\varepsilon(1/2+it)| \leq C_2 \exp[-|1/2+it|^\beta] = C_2 e^{-(1/4+t^2)^{\beta/2}},$$

we obtain

$$(B.10) \quad \sup_{u \in [1/2, 1]} |\mathcal{H}f_\varepsilon(1/2+i\delta u)| \leq C_2 e^{-(1/4+\delta^2/4)^{\beta/2}} \leq C_2 e^{-(\delta/2)^\beta}.$$

It follows from (B.8), (B.9) and (B.10) that there is a constant $C > 0$ such that

$$\begin{aligned}\int |f_\varepsilon * H^\delta|^2 &= \int |\mathcal{H}H^\delta(1/2+it)|^2 |\mathcal{H}f_\varepsilon(1/2+it)|^2 d\tau \\ &\asymp \int_{1/2}^1 \delta^{-2} |\mathcal{H}H(1/2+iu)|^2 |\mathcal{H}f_\varepsilon(1/2+i\delta u)|^2 (\delta u) \tanh(\pi\delta u) \delta du \\ &\leq C e^{-2(\delta/2)^\beta}.\end{aligned}$$

This completes the proof of Lemma B.5. \square

B.3.3. *Bound on $g_0 = f_\varepsilon * f_0$.* Choose f_0 as

$$f_0(k(e^{-r}i)) = f_0(e^{-r}i) = \frac{a-1}{2\pi}(\cosh r)^{-a} \quad \text{for } a > 1.$$

LEMMA B.6. *f_0 is $\mathbb{S}\mathbb{O}(2)$ -invariant and*

$$\int_{r=0}^{\infty} \int_{u=0}^{2\pi} f_0(k_u(e^{-r}i)) \sinh r \, dr \, du = 1.$$

PROOF. By the definition of f_0 , it is $\mathbb{S}\mathbb{O}(2)$ -invariant and

$$\begin{aligned} & \int_{r=0}^{\infty} \int_{u=0}^{2\pi} f_0(k_u(e^{-r}i)) \sinh r \, dr \, du \\ &= (a-1) \int_{r=0}^{\infty} (\cosh r)^{-a} \sinh r \, dr \\ &= (a-1) \int_{x=1}^{\infty} x^{-a} \, dx = 1. \end{aligned} \quad \square$$

LEMMA B.7. *Suppose that f_ε is bi-invariant and*

$$\int_0^{C_\varepsilon} f_\varepsilon(e^{-s}i) \sinh s \, ds \geq \frac{1}{2}$$

for some positive constant C_ε . Then, $g_0 = f_\varepsilon * f_0$ satisfies

$$g_0(e^{-r}i) \geq \begin{cases} 2\pi(a-1)2^{a-1}e^{-2ar}, & \text{for } r > C_\varepsilon, \\ 2\pi(a-1)2^{a-1}e^{-2aC_\varepsilon}, & \text{for } r \leq C_\varepsilon. \end{cases}$$

PROOF. Note that $0 \leq s \leq C_\varepsilon < r$ implies $r+s \leq 2r$ whereas $0 \leq s, r \leq C_\varepsilon$, implies $r+s \leq 2C_\varepsilon$. It follows from these facts, $f_\varepsilon \geq 0$, Lemmas B.2 and B.3 that

$$\begin{aligned} & f_\varepsilon * f_0(e^{-r}i) \\ &= 2\pi \int_0^{2\pi} \int_0^\infty f_\varepsilon(e^{-s}i) f_0(k_{\eta(r,s,\phi)} e^{-R(r,s,\phi)}i) \sinh s \, ds \, d\phi \\ &= (a-1) \int_0^{2\pi} \int_0^\infty f_\varepsilon(e^{-s}i) \cosh^{-a}(R(r,s,\phi)) \sinh s \, ds \, d\phi \\ &\geq 2\pi(a-1) \int_0^{C_\varepsilon} f_\varepsilon(e^{-s}i) \cosh^{-a}(r+s) \sinh s \, ds \\ &\geq \frac{a-1}{\cosh^a(2\tau)} \int_0^{C_\varepsilon} f_\varepsilon(e^{-s}i) \sinh s \, ds \\ &\geq 2\pi \frac{a-1}{2 \cosh^a(2\tau)} \geq 2\pi(a-1)2^{a-1}e^{-2a\tau} \end{aligned}$$

with $\tau = r$ for $r > C_\varepsilon$ and $\tau = C_\varepsilon$ for $r \leq C_\varepsilon$. \square

B.3.4. *Bound on $f_\varepsilon * H^\delta$.* We note from [30], page 188,

$$P_{-1/2}(\cosh r) = \frac{2}{\pi \cosh(r/2)} K(\tanh(r/2)),$$

where the complete elliptic integral of the first kind is defined by

$$K(t) = \int_0^{\pi/2} \frac{d\phi}{\sqrt{1-t^2 \sin^2 \phi}}.$$

In consequence there is a $C > 0$ such that for all $r > 0$

$$(B.11) \quad P_{-1/2}(\cosh r) \leq C.$$

Define

$$\mu_\delta(e^{-r}i) = \delta e^{-(m_0-1)\delta r} \quad \text{for } r \geq 0.$$

When $m_0 > 1$ and $\delta > 0$, $\|\mu_\delta\|_\infty \leq \delta$ and $\mu_\delta(e^{-r}i)$ is monotonically decreasing in r .

LEMMA B.8. *Suppose $|H(e^{-r}i)| \leq C e^{-m_0 r}$ with $m_0 > 1$ and $\delta \geq 1$. Then, there is a constant $C > 0$ such that $H^\delta(e^{-r}i) \leq C \mu_\delta(e^{-r}i)$.*

PROOF. By Taylor's expansion,

$$(e^r)^\delta - (e^{-r})^\delta = \delta \eta^{\delta-1} (e^r - e^{-r})$$

for $e^{-r} \leq \eta \leq e^r$. Since $\eta^{\delta-1} \leq e^{(\delta-1)r} \leq e^{\delta r}$,

$$\frac{\sinh(\delta r)}{\sinh r} \leq \delta e^{\delta r} \quad \text{for } r \geq 0.$$

Hence with $C > 0$ from (B.11),

$$\begin{aligned} |H^\delta(e^{-r}i)| &= |H(e^{-\delta r}i)| \frac{\sinh(\delta r)}{\sinh r} P_{-1/2}(\cosh(\delta r)) \\ &\leq C |H(e^{-\delta r}i)| \frac{\sinh(\delta r)}{\sinh r} \leq C e^{-m_0 \delta r} \delta e^{\delta r} = C \mu_\delta(e^{-r}i). \quad \square \end{aligned}$$

LEMMA B.9. *Suppose that*

$$\int_{r-\xi_0 r}^{r+\xi_0 r} f_\varepsilon(e^{-s}i) \sinh s \, ds \leq C e^{-(\xi-\xi_0)r} \quad \text{for } 0 < \xi_0 < 1 \text{ and } \xi > 1 + \xi_0,$$

$H(e^{-r}i)$ is bounded and monotonely decreasing in r and satisfies the tail condition

$$(B.12) \quad H(e^{-r}i) \leq C e^{-m_0 r} \quad \text{for } m_0 \xi_0 > \xi.$$

Then, for $\delta \geq 1$ and $r > 0$,

$$(f_\varepsilon * H^\delta)(e^{-r}i) \leq C \delta e^{-(\xi-\xi_0)r}.$$

PROOF. Set $\mathcal{R}_1 = \{s : |r-s| \leq \xi_0 r\}$ and $\mathcal{R}_2 = \{s : |r-s| > \xi_0 r\}$. It follows from Lemmas B.2, B.4 and B.8 that

$$\begin{aligned}
& \frac{1}{2\pi} (f_\varepsilon * H^\delta)(e^{-r}i) \\
&= \int_{\phi=0}^{2\pi} \int_{s=0}^{\infty} f_\varepsilon(e^{-s}i) H^\delta(k_{\eta(r,s,\phi)} e^{-R(r,s,\phi)}i) \sinh s \, d\phi \, ds \\
&\leq C \int_{\phi=0}^{2\pi} \int_{s=0}^{\infty} f_\varepsilon(e^{-s}i) \mu_\delta(e^{-R(r,s,\phi)}i) \sinh s \, d\phi \, ds \\
\text{(B.13)} \quad &\leq 2\pi C \int f_\varepsilon(e^{-s}i) \mu_\delta(e^{-|r-s|}i) \sinh s \, ds.
\end{aligned}$$

Set

$$I_j = \int_{\mathcal{R}_j} f_\varepsilon(e^{-s}i) \mu_\delta(e^{-|r-s|}i) \sinh s \, ds \quad \text{for } j = 1, 2.$$

Since $m_0 > \xi/\xi_0 > 1$,

$$\|\mu_\delta\|_\infty \leq \delta.$$

Observe that

$$\begin{aligned}
I_1 &\leq \|\mu_\delta\|_\infty \int_{|r-s| \leq \xi_0 r} f_\varepsilon(e^{-s}i) \sinh s \, ds \\
\text{(B.14)} \quad &\leq C \delta e^{-(\xi-\xi_0)r}.
\end{aligned}$$

From the tail condition (B.12),

$$\begin{aligned}
I_2 &= \int_{|r-s| > \xi_0 r} f_\varepsilon(e^{-s}i) (\delta e^{-(m_0-1)\delta|r-s|}) \sinh s \, ds \\
&\leq \delta e^{-(m_0-1)\delta\xi_0 r} \int_{|r-s| > \xi_0 r} f_\varepsilon(e^{-s}i) \sinh s \, ds \\
\text{(B.15)} \quad &\leq \delta e^{-(m_0-1)\delta\xi_0 r}.
\end{aligned}$$

Since $r \geq 0$, $m_0\xi_0 > \xi$ and δ is large,

$$\frac{e^{-(\xi-\xi_0)r}}{e^{-(m_0-1)\delta\xi_0 r}} = e^{(m_0-1)\delta\xi_0 r - (\xi-\xi_0)r} \geq e^{(m_0-1)\xi_0 r - (\xi-\xi_0)r} = e^{(m_0\xi_0 - \xi)r} \geq 1.$$

Combining (B.13), (B.14), (B.15), we have the desired result. \square

B.3.5. *Chi-square distance: Proof of (B.6).* With the above notation, choose a pair of densities

$$f_0(k(e^{-r}i)) = f_0(e^{-r}i) = \frac{a-1}{2\pi}(\cosh r)^{-a} \quad \text{and} \quad f_n = f_0 + C_H \delta^{-\alpha} H^\delta,$$

where a satisfies $1 < a < 2$, and H satisfies the hypotheses of Lemmas B.5 and B.9. By choosing C_H close to 0, we have $f_0, f_n \in \mathcal{F}_\alpha(Q)$ for all large δ . Let $g_0 = f_\varepsilon * f_0$ and $g_n = f_\varepsilon * f_n$ with f_ε satisfying the hypotheses of Lemma B.9 and (D.4) with $\gamma = 1$.

The χ^2 distance between g_0 and g_n is defined by

$$\chi^2(g_0, g_n) := \int \frac{(g_n - g_0)^2}{g_0} dz = 2\pi C_H^2 \delta^{-2\alpha} \int \frac{(f_\varepsilon * H^\delta(e^{-r}i))^2}{g_0(e^{-r}i)} \sinh r dr$$

and with a suitable constant $M > 0$ guaranteed by Lemma B.7, by Lemmas B.5, B.8 and B.9

$$\begin{aligned} & \int \frac{(f_\varepsilon * H^\delta(e^{-r}i))^2}{g_0(e^{-r}i)} \sinh r dr \\ & \leq \left(\int_{e^r \leq M} + \int_{e^r > M} \right) \frac{(f_\varepsilon * H^\delta(e^{-r}i))^2}{g_0(e^{-r}i)} \sinh r dr \\ & \leq \frac{M^{2a}}{C} \int (f_\varepsilon * H^\delta(e^{-r}i))^2 \sinh r dr + \frac{\delta^2}{C} \int_{e^r > M} \frac{e^{-2(\xi-\xi_0)r}}{e^{-2ar}} \sinh r dr \\ & = O(M^{2a} e^{-2(\delta/2)^\beta} + \delta^2 M^{-2(\xi-\xi_0)+2a+1}) = O(e^{-\mu_1(\delta/2)^\beta}), \end{aligned}$$

where $C = 2\pi(a-1)2^{a-1}$. For the last equality we set $M = e^{1/2(\delta/2)^\beta}$, $\mu_0 = 2(\xi - \xi_0) - 2a - 1$ and $\mu_1 = \min(\mu_0/2, (2-a))$. Then indeed

$$M^{2a} e^{-2(\delta/2)^\beta} = e^{-(2-a)(\delta/2)^\beta} = O(e^{-\mu_1 \delta^\beta}) \quad \text{and} \quad \delta^2 M^{-\mu_0} = O(e^{-\mu_1 \delta^\beta}).$$

Hence,

$$(B.16) \quad \chi^2(g_0, g_n) = O(\delta^{-2\alpha} e^{-\mu_1(\delta/2)^\beta}).$$

Letting $e^{-\mu_1(\delta/2)^\beta} = n^{-1}$, or equivalently

$$(B.17) \quad \delta = 2\mu_1^{-1/\beta} (\log n)^{1/\beta},$$

we conclude that the right-hand side of (B.16) is of order $o(n^{-1})$, that is, (B.6) is proven.

Acknowledgments. The authors would like to express their sincerest gratitude to the late Dennis M. Healy Jr. (1957–2009), whose untimely death was most unfortunate. The second author had been in conversations with him about this very problem for over twenty years, and he has passed away prior to seeing the completion of this remarkable problem. For this and so much more, we are all grateful.

REFERENCES

- [1] ABRAMOVICH, F. and SILVERMAN, B. (1998). Wavelet decomposition approaches to statistical inverse problems. *Biometrika* **85** 115–129. [MR1627226](#)
- [2] ALLEN, J. C. and HEALY JR., D. M. (2003). Hyperbolic geometry, Nehari’s theorem, electric circuits, and analog signal processing. *Modern Signal Processing* **46** 1–62.
- [3] BHATTACHARYA, R. and PATRANGENARU, V. (2003). Large sample theory of intrinsic and extrinsic sample means on manifolds I. *Ann. Statist.* **31** 1–29. [MR1962498](#)
- [4] BHATTACHARYA, R. and PATRANGENARU, V. (2005). Large sample theory of intrinsic and extrinsic sample means on manifolds II. *Ann. Statist.* **33** 1225–1259. [MR2195634](#)
- [5] BISSANTZ, N., HOHAGE, T., MUNK, A. and RUYMGAART, F. (2007). Convergence rates of general regularization methods for statistical inverse problems and applications. *SIAM J. Numer. Anal.* **45** 2610–2636. [MR2361904](#)
- [6] BROWN, B. H. (2001). Medical impedance tomography and process impedance tomography: A brief review. *Meas. Sci. Technol.* **12** 991–996.
- [7] BUTUCEA, C. and TSYBAKOV, A. (2007). Sharp optimality for density deconvolution with dominating bias, I; II. *Theory Probab. Appl.* **52** 111–128; 336–349. [MR2354572](#)
- [8] CAVALIER, L., GOLUBEV, G., LEPSKI, O. and TSYBAKOV, A. (2003). Block thresholding and sharp adaptive estimation in severely ill-posed inverse problems. *Theory Probab. Appl.* **48** 534–556. [MR2141349](#)
- [9] CAVALIER, L., GOLUBEV, G., PICARD, D. and TSYBAKOV, A. (2002). Oracle inequalities for inverse problems. *Ann. Statist.* **30** 843–874. [MR1922543](#)
- [10] COLLIN, R. E. (1992). *Foundations for Microwave Engineering*. McGraw-Hill, New York.
- [11] DELAIGLE, A. and GIJBELS, I. (2004). Practical bandwidth selection in deconvolution kernel density estimation. *Comput. Statist. Data Anal.* **45** 249–267. [MR2045631](#)
- [12] DELAIGLE, A., HALL, P. and MEISTER, A. (2008). On deconvolution with repeated measurements. *Ann. Statist.* **36** 665–685. [MR2396811](#)
- [13] DEY, A., MAIR, B. and RUYMGAART, F. (1996). Cross-validation for parameter selection in inverse estimation problems. *Scand. J. Statist.* **23** 609–620. [MR1439715](#)
- [14] EWART, G., MILLS, K., COX, G. and GAGE, P. (2002). Amiloride derivatives block ion channel activity and enhancement of virus-like particle budding caused by HIV-1 protein Vpu. *Eur. Biophys. J.* **31** 26–35.
- [15] FAN, J. (1991). On the optimal rates of convergence for nonparametric deconvolution problem. *Ann. Statist.* **19** 1257–1272. [MR1126324](#)
- [16] GOLDENSHLUGER, A. (1999). On pointwise adaptive nonparametric deconvolution. *Bernoulli* **5** 907–926. [MR1715444](#)
- [17] HAHN, G., JUST, A., DITTMAR, J. and HELBIG, G. (2008). Systematic errors of EIT systems determined by easily-scalable resistive phantoms. *Physiol. Meas.* **29** 163–172.
- [18] HALL, P. and MEISTER, A. (2007). A ridge-parameter approach to deconvolution. *Ann. Statist.* **35** 1535–1558. [MR2351096](#)
- [19] HALL, P. and QIU, P. (2005). Discrete-transform approach to deconvolution problems. *Biometrika* **92** 135–148. [MR2158615](#)
- [20] HELTON, J. W. (1982). Non-Euclidean functional analysis and electronics. *Bull. Amer. Math. Soc. (N.S.)* **7** 1–64. [MR0656197](#)
- [21] JOHNSTONE, I. M., KERKYACHARIAN, G., PICARD, D. and RAIMONDO, M. (2004). Wavelet deconvolution in a periodic setting. *J. R. Stat. Soc. Ser. B Stat. Methodol.* **66** 547–573. [MR2088290](#)

- [22] JOHNSTONE, I. M. and RAIMONDO, M. (2004). Periodic boxcar deconvolution and Diophantine approximation. *Ann. Statist.* **32** 1781–1804. [MR2102493](#)
- [23] JOHNSTONE, I. M. and SILVERMAN, B. W. (1991). Discretization effects in statistical inverse problems. *J. Complexity* **7** 1–34. [MR1096170](#)
- [24] KALIFA, J. and MALLAT, S. (2003). Thresholding estimators for linear inverse problems and deconvolutions. *Ann. Statist.* **31** 58–109. [MR1962500](#)
- [25] KASS, R. E. and VOS, P. W. (1997). *Geometrical Foundations of Asymptotic Inference*. Wiley, New York. [MR1461540](#)
- [26] KERKYACHARIAN, G., PETRUSHEV, P., PICARD, D. B. and WILLER, T. (2007). Needlet algorithms for estimation in inverse problems. *Electron. J. Stat.* **1** 30–76. [MR2312145](#)
- [27] KIM, P. T. and KOO, J.-Y. (2005). Statistical inverse problems on manifolds. *J. Fourier Anal. Appl.* **11** 639–653. [MR2190676](#)
- [28] KIM, P. T. and RICHARDS, D. S. (2001). Deconvolution density estimation on compact Lie groups. In *Algebraic Methods in Statistics and Probability (Notre Dame, IN, 2000)*. *Contemporary Mathematics* **287** 155–171. Amer. Math. Soc., Providence, RI. [MR1873674](#)
- [29] KIM, P. T. and RICHARDS, D. S. (2008). Diffusion tensor imaging and deconvolution on the space of positive definite symmetric matrices. In *Mathematical Foundations of Computational Anatomy: Geometric and Statistical Methods for Biological Shape Variability Modeling* (X. Pennec and S. Joshi, eds.) 140–149. Available at <http://www-sop.inria.fr/asclepios/events/MFCA08/Proceedings/MFCA08.Proceedings.pdf>.
- [30] LEBEDEV, N. (1972). *Special Functions and Their Applications*. Dover, New York. [MR0350075](#)
- [31] LEE, J. M. (1997). *Riemannian Manifolds: An Introduction to Curvature*. Springer, New York. [MR1468735](#)
- [32] LOVRIC, M., MIN-OO, M. and RUH, E. A. (2000). Multivariate normal distributions parametrized as a riemannian symmetric space. *J. Multivariate Anal.* **74** 36–48. [MR1790612](#)
- [33] MAIR, B. A. and RUYMGAART, F. H. (1996). Statistical inverse estimation in Hilbert scales. *SIAM J. Appl. Math.* **56** 1424–1444. [MR1409127](#)
- [34] MCCULLAUGH, P. (1992). Conditional inference and cauchy models. *Biometrika* **79** 247–259. [MR1185127](#)
- [35] MCCULLAUGH, P. (1996). Möbius transformation and Cauchy parameter estimation. *Ann. Statist.* **24** 787–808. [MR1394988](#)
- [36] MIZERA, I. and MÜLLER, C. (2004). Location-scale depth (with discussion). *J. Amer. Statist. Assoc.* **99** 949–966. [MR2109488](#)
- [37] NEUBAUER, A. (2008). The convergence of a new heuristic parameter selection criterion for general regularization methods. *Inverse Problems* **24** 055005. [MR2438940](#)
- [38] NEVANLINNA, R. and PAATERO, V. (1964). *Einführung in die Funktionentheorie*. Birkhäuser, Basel.
- [39] PENSKY, M. and SAPATINAS, T. (2009). Functional deconvolution in a periodic setting: Uniform case. *Ann. Statist.* **37** 73–104. [MR2488345](#)
- [40] PEREVERZEV, S. and SCHOCK, E. (2005). On the adaptive selection of the parameter in regularization of ill-posed problems. *SIAM J. Numer. Anal.* **43** 2060–2076. [MR2192331](#)

- [41] RÖMER, W. and STEINEM, C. (2004). Impedance analysis and single-channel recordings on nano-black lipid membranes based on porous alumina. *Biophys. J.* **86** 955–965.
- [42] SZKUTNIK, Z. (2003). Doubly smoothed EM algorithm for statistical inverse problems. *J. Amer. Statist. Assoc.* **98** 178–190. [MR1965684](#)
- [43] TERRAS, A. (1985). *Harmonic Analysis on Symmetric Spaces and Applications*. I. Springer, New York. [MR0791406](#)
- [44] VAN ES, B., GUGUSHVILI, S. and SPREIJ, P. (2008). Deconvolution for an atomic distribution. *Electron. J. Stat.* **2** 265–297. [MR2399196](#)
- [45] WAND, M. P. and JONES, M. C. (1994). *Kernel Smoothing*. Chapman and Hall, London. [MR1319818](#)

S. F. HUCKEMANN
A. MUNK
INSTITUT FÜR MATHEMATISCHE STOCHASTIK
GEORG-AUGUST-UNIVERSITÄT GÖTTINGEN
GOLDSCHMIDTSTR. 7
D-37077 GÖTTINGEN
GERMANY
E-MAIL: huckeman@math.uni-goettingen.de
munk@math.uni-goettingen.de

P. T. KIM
DEPARTMENT OF MATHEMATICS
AND STATISTICS
UNIVERSITY OF GUELPH
GUELPH, ONTARIO N1G 2W1
CANADA
E-MAIL: pkim@uoguelph.ca

J.-Y. KOO
DEPARTMENT OF STATISTICS
KOREA UNIVERSITY
ANAM-DONG SUNGBUK-KU
SEOUL 136-701
KOREA
E-MAIL: jykoo@korea.ac.kr